



1 **Discovery of reactive chlorine, sulphur and nitrogen**
2 **containing ambient volatile organic compounds in the megacity**
3 **of Delhi during both clean and extremely polluted seasons**

4 Sachin Mishra¹, Vinayak Sinha¹, Haseeb Hakkim¹, Arpit Awasthi¹, Sachin D. Ghude², Vijay
5 Kumar Soni³, Narendra Nigam³, Baerbel Sinha¹, Madhavan N. Rajeevan⁴

6 ¹ Department of Earth and Environmental Sciences, Indian Institute of Science Education and Research Mohali,
7 Sector 81, S.A.S Nagar, Manauli PO, Punjab, 140306, India

8 ² Indian Institute of Tropical Meteorology, Pashan, Pune 411 008, Ministry of Earth Sciences, India

9 ³ India Meteorological Department, New Delhi 110 003, India, Ministry of Earth Sciences, India

10 ⁴ Ministry of Earth Sciences, Government of India, New Delhi 110 003, India

11 * Correspondence to: Vinayak Sinha (vsinha@iisermohali.ac.in)

12 **Abstract.** Volatile organic compounds significantly impact the atmospheric chemistry of polluted megacities.
13 Delhi is a dynamically changing megacity and yet our knowledge of its ambient VOC composition and chemistry
14 is limited to few studies conducted mainly in winter before 2020 (all pre-covid). Here, using a new extended
15 volatility range high mass resolution (10000-15000) Proton Transfer Reaction Time of Flight Mass
16 Spectrometer10K, we measured and analyzed ambient VOC-mass spectra acquired continuously over a four-
17 month period covering “clean” monsoon (July-September) and “polluted” post-monsoon seasons, for the year
18 2022. Out of 1126 peaks, 111 VOC species were identified unambiguously. Averaged total mass concentrations
19 reached $\sim 260 \mu\text{g m}^{-3}$ and were >4 times in polluted season relative to cleaner season, driven by enhanced emissions
20 from biomass burning and reduced atmospheric ventilation (~ 2). Among 111, 56 were oxygenated, 10 contained
21 nitrogen, 2 chlorine, 1 sulphur and 42 were pure hydrocarbons. VOC levels during polluted periods were
22 significantly higher than most developed world megacities. Surprisingly, methanethiol, dichlorobenzenes, C6-
23 amides and C9-organic acids/esters, which have previously never been reported in India, were detected in both
24 the clean and polluted periods. The sources were industrial for methanethiol and dichlorobenzenes, purely
25 photochemical for the C6-amides and multiphase oxidation and partitioning for C9-organic acids. Aromatic
26 VOC/CO emission ratio analyses indicated additional biomass combustion/industrial sources in post-monsoon
27 season, alongwith year-round traffic sources in both seasons. Overall, the unprecedented new information
28 concerning ambient VOC speciation, abundance, variability and emission characteristics during contrasting
29 seasons significantly advances current atmospheric composition understanding of highly polluted urban
30 atmospheric environments like Delhi.

31

32 **1 Introduction**

33 The national capital territory of Delhi is jointly administered by the central and state governments and
34 accommodated more than 32 million people in 2022. For the past several years, its population has grown at the
35 rate of more than 2.7 percent per year, adding about 1 million new inhabitants each year. Thus, the region
36 represents a complex dynamically changing emission environment driven by rapid changes in emissions as



37 regulatory authorities make efforts to improve urban infrastructure and public transportation while promoting
38 cleaner technologies. As a megacity in a developing country with one of the world's highest population densities,
39 Delhi exemplifies some of the key challenges faced by many megacities in the global south, where increased
40 urbanization and inequitable access to clean energy sources along with unfavourable meteorological conditions
41 during cold periods of the year, cause the inhabitants to suffer from extreme air pollution episodes. Lelieveld et
42 al. (2015) identified South Asia as one of the global air pollution hotspots in terms of the contribution of outdoor
43 air pollution sources to premature mortality due to particulate matter pollution. Reduction of other atmospheric
44 pollutants is also deemed necessary to fulfil the UN Sustainable Development Goals (Keywood et al., 2023). Thus,
45 the study of Delhi's ambient chemical composition using state of the art technology can offer valuable insights
46 and lessons for our understanding of polluted atmospheric environments.

47 Previous studies have demonstrated that air pollution in the Delhi-NCR metropolitan area peaks during the post-
48 monsoon (October- November) season (e.g. Kulkarni et al., 2020), coinciding with the time of year when large
49 scale paddy stubble burning occurs in the Indo-Gangetic Plain (Kumar et al., 2021). The main air pollutant in
50 exceedance has long been identified to be particulate matter (e.g. PM_{2.5}) and many studies (Gani et al., 2020; Cash
51 et al., 2021; Sharma et al., 2023; Singh et al., 2011) have documented the variability, exceedance and composition
52 of aerosols. Volatile organic compounds (VOCs) are major precursors of secondary organic aerosol, which is a
53 significant component of PM_{2.5} (30-60% in Delhi; Chen et al., 2022; Nault et al., 2021) and surface ozone over
54 Delhi. In fact, in-situ ozone production in Delhi has been reported to be more sensitive to VOCs rather than
55 nitrogen oxides (Nelson et al., 2021). Several VOCs (e.g. benzene, nitromethane, 1,3-butadiene) are also
56 carcinogenic (WHO 2010) at high exposure concentrations and many pose direct health risks (Ho et al., 2006;
57 Espenship et al., 2019; WHO 2019; Weng et al., 2009; Roberts et al., 2011; Durmusoglu et al., 2010). VOCs can
58 also aid source apportionment studies by acting as source fingerprints and valuable molecular markers of specific
59 emission sources (de Gouw et al., 2017; Holzinger et al., 1999; Warneke et al., 2001; Kumar et al., 2020; Garg et
60 al., 2016; Hakkim et al., 2021; Kumar et al., 2021). In the complex emission environment of cities in the developing
61 world, this can be especially helpful since the energy usage portfolio is such that biomass burning sources are
62 likely to be as significant as fossil-fuel based sources (Bikkina et al., 2019) in influencing the air pollutant burden
63 of VOCs, resulting in ambient air VOC composition that could be quite different from cities like Los Angeles
64 (McDonald et al., 2018).

65 Existing knowledge about the abundance and diurnal variability of major ambient VOCs such as methanol,
66 acetone, acetaldehyde, acetonitrile, isoprene, benzene, toluene, xylenes and trimethyl benzenes in Delhi, is limited
67 to just four previously measured wintertime datasets: Dec-March of 2016 (Chandra et al., 2018; Hakkim et al.,
68 2019), Dec-March of 2018 (Wang et al., 2020; Tripathi et al., 2022), few days in October 2018 (Nelson et al.,
69 2021; Bryant et al., 2023) and one spanning 145 days of 2019 that reported source apportionment of some VOCs
70 for different seasons (Jain et al., 2022). We note that all these were pre-COVID period datasets, and that since
71 these observations many new regulations have been put in place e.g. for traffic with the introduction of BS-VI
72 (EURO6 equivalent) in 2020 and the FAME program for promotion of E-vehicles, and for industries with a ban
73 on the use of petcoke in the NCR and the crackdown on unregistered industries (Guttikunda et al., 2023). The
74 monsoon season which precedes the post-monsoon season lasts from June to September and is characterized by
75 better air quality, aided by favourable meteorological conditions, including higher ventilation co-efficient,
76 negligible agricultural waste burning and enhanced wet scavenging (Kumar et al., 2016).

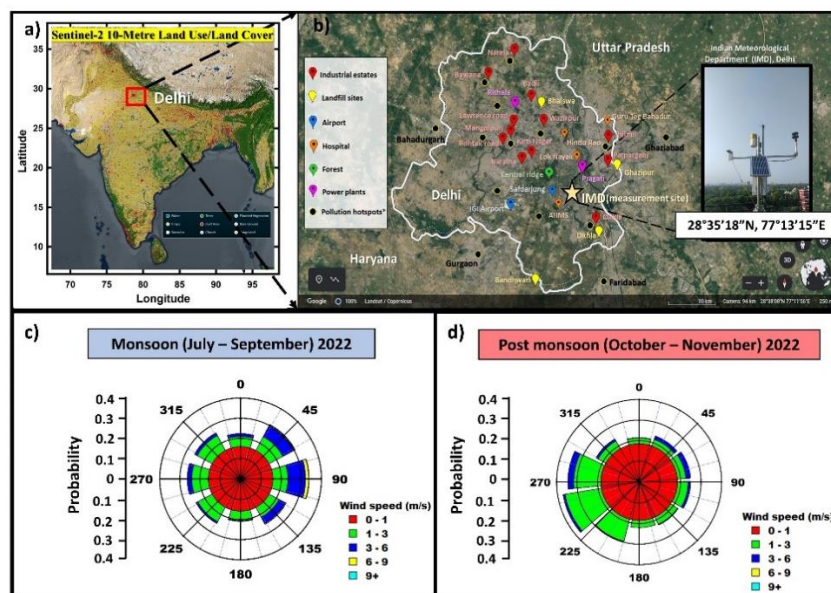


77 This study addresses some of the above knowledge gaps pertaining to ambient VOCs during the “clean” monsoon
78 season characterized by baseline pollution levels and the polluted “post-monsoon” season characterized by
79 extreme pollution events and large scale open agricultural biomass waste fires regionally. Employing a new
80 extended volatility range (EVR) high mass resolution (10000-15000) Proton Transfer Reaction Time of Flight
81 Mass Spectrometer 10K (PTR-TOF 10000; Ionicon Analytik GmbH), a technology that has never before been
82 deployed in India, we investigated the ambient VOC speciation, abundance, variability and emission
83 characteristics in the polluted urban environment of Delhi over a 4-month period. This enabled us to discover
84 several low volatility VOCs, many of which are present in fire emissions (Koss et al., 2018), for the time in South
85 Asia, as all previous VOC studies have involved either the older PTR-TOF-MS or PTR-QMS instruments, that
86 have significantly lower mass resolution and lower detection sensitivity and did not possess the extended volatility
87 range components. We first undertook comprehensive and rigorous interpretation of the ambient mass spectra
88 over a four-month period spanning July-Nov of 2022 in Delhi. This was followed by identification and
89 quantification of 111 VOCs, many of which have been discovered and reported for the first time from the South
90 Asian atmospheric environment. Each of these compounds was then classified in terms of oxygenated VOCs, pure
91 hydrocarbons, major nitrogen containing VOCs, chlorine containing VOCs and sulphur containing VOCs,
92 followed by the time series analyses and diurnal profiles of the major VOCs and some new/rarely reported VOCs
93 in both seasons as a function of meteorology and emissions. The atmospheric chemistry implications of some of
94 the newly discovered compounds in this polluted urban environment are discussed. Further, using measured
95 aromatic VOC/CO emission ratios in monsoon and post-monsoon season, a global comparison with reports from
96 megacities in Europe, North America and Asia was undertaken for a nuanced understanding of their levels and
97 sources in Delhi relative to megacities across these different continents.

98 **2. Methodology**

99 **2.1 Measurement site and meteorological conditions:**

100



101

102 **Figure 1:** Map of India showing Delhi (1 a) and zoom in of the measurement site (1b; Google Earth
103 Imagery © Google Earth) with a view from the roof-top of the SatMet Building (28.5896°N-77.2210°E), and wind rose
104 plots derived from in-situ one-minute wind speed and wind direction data during monsoon (1c) and post-monsoon
105 (1d) 2022 acquired at sampling height of ~35m A.G.L

106

107 The measurement site was located within the premises of the India Meteorological Department (IMD) which is
108 situated in Central Delhi (Fig. 1). Ambient air was sampled at a height of circa 35m above ground level from
109 the roof-top of the SatMet building (28.5896°N-77.2210°E), into the instruments which were housed inside a
110 laboratory located in the sixth floor of the same building.

111 Figure 1 (a) shows the land use/ land cover (Sentinel-2 10m) map of India with a red marked box highlighting
112 Delhi. The city is bordered on its northern, western, and southern sides by the state of Haryana and to the east by
113 the state of Uttar Pradesh. The star marked in Fig. 1 (b) shows the measurement site (IMD Delhi) and its
114 surroundings. The major pollution hotspots include places like Ghaziabad (towards the northeast), Bahadurgarh
115 (towards the northwest), Gurgaon (towards the southwest), and Faridabad and Okhla (towards the southeast),
116 which are highlighted as black dots. The industrial areas are marked in red (e.g. Okhla industrial area), while
117 major landfill sites are marked in yellow. The international airport is marked with a blue pointer. Major hospitals
118 are marked in orange, forest areas in green, and power plants are marked in sky-blue colour.

119 Meteorological sensors (Campbell Scientific Inc.) were deployed to measure the wind speed, direction,
120 temperature, relative humidity and photosynthetic active radiation (model nos.: CS215 for temperature and RH,
121 PAR PQSI sensor, and for rain TE525-L40). Boundary layer height was taken from ERA5 reanalyses dataset
122 (Hersbach et al., 2023) and ventilation coefficient was calculated as the product of the measured wind speed and
123 boundary layer height. Figures 1 (c) and 1 (d) show the wind rose plot derived from the in-situ one-minute wind
124 speed and wind direction data acquired at the measurement site for monsoon (July 2022 – September 2022) and
125 post-monsoon (October 2022 – November 2022) seasons, respectively. The prevalent wind direction changed



126 from easterly flow in monsoon season to westerly flow in the post-monsoon season. During the monsoon season,
127 the major fetch region spanned from the NE to SE-E. These NE, E, and SE winds were associated with high wind
128 speeds ranging from 3 – 6 ms⁻¹, which on occasions reached up to 9 ms⁻¹. During the post-monsoon season, the
129 major wind flow was from the NW to the SW-W sector. These wind speeds were lower, ranging from 1 – 3 ms⁻¹
130 exceeding 6 ms⁻¹ only occasionally. Overall, the site received air from all wind sectors in both seasons. This is
131 also borne by the back trajectory analyses presented in the companion paper (Awasthi et al., 2024), which showed
132 that the site is characterized by regional airflow patterns as documented at other sites in the Indo-Gangetic Plain
133 (Pawar et al., 2015).

134 Fire count data were obtained using the Visible Infrared Imaging Radiometer Suite (VIIRS) 375m thermal
135 anomalies/active fire product data from the VIIRS sensor aboard the joint NASA/NOAA Suomi National Polar-
136 orbiting Partnership (Suomi NPP) and NOAA-20 satellites for high and normal confidence intervals only.

137 **2.2 Measurement of Volatile Organic Compounds using the PTR-TOF-MS 10K**

138 Volatile organic compounds (VOCs) were measured using a new high sensitivity and high mass resolution Proton
139 Transfer Reaction Time of Flight Mass Spectrometer (PTR-TOF-MS 10k, model PT10-004 manufactured by
140 Ionicon Analytik GmbH, Austria). While PTR-TOF-MS 8000 series (Tripathi et al., 2022) and PTR-QMS (Sinha
141 et al., 2014) instruments have been previously deployed in India and have mass resolutions of 8000 and 1,
142 respectively, this study marks the first deployment of the PTR-TOF-MS 10K system in India, a system that
143 possesses several unique advantages over the older generation instruments for VOC measurements in polluted
144 and complex emission environments. The first is that this new system is equipped with the extended volatility
145 range technology (Piel et al., 2021), ensuring that even many intermediate volatility range compounds and sticky
146 VOCs can be detected with very fast response times and minimal surface effects. The inlet system of the
147 instrument as well as the ionization chamber is fully built into a heated chamber and the inlet capillary is further
148 fed through a heated hose to ensure there are no “cold” spots for condensation. The entire inlet system is made of
149 inert material (e.g. PEEK or siliconert treated steel capillaries to keep surface effects minimal. Additionally, a 7
150 μm siliconert filter just before the drift tube served to minimize clogging/contamination of the system. The second
151 advantage possessed by the PTR-TOF-10K used in this work is the inclusion of an ion booster funnel and hexapole
152 ion guide placed after the drift tube/reaction chamber for improved extraction of ions in a manner that boosts both
153 the mass resolution as well as the sensitivity over its older peers. This helped achieve much higher mass resolution
154 (> 10000 m/Δm), even reaching as high as 15000 m/Δm at m/z 330, and detection limits better than 3 ppt for all
155 compounds detected in the mass to charge ratio (m/z) 31-330 mass range. These customizations over previously
156 deployed PTR-TOF-MS instruments in Delhi, enabled detection and discovery of several intermediate range-
157 volatility compounds (IVOCs) in the gas phase. Other parts of the instrument consisted of proven PTR-TOF-MS
158 technology in the form of a hollow cathode ion source, which produces a stream of pure H₃O⁺ through the plasma
159 discharge of water vapour, the reaction chamber/drift tube where the VOCs (Analyte molecules) having proton
160 affinity higher than that of H₂O (164.8 kcal mol⁻¹) underwent primarily soft chemical ionization typically forming
161 the corresponding protonated molecular ions. At the end of the lens system, the ions entered the pulser region
162 through an aperture and were accelerated in the TOF region (Time of Flight), a field-free region where the ions
163 rebounded in a reflectron and were refocused and detected using a Multi-Channel Plate (MCP) detector (Burle
164 Industries Inc., Lancaster, PA, USA.). These aspects of the PTR-TOF-MS technology have already been explained



165 well earlier (Jordan et al., 2009; Graus et al., 2010). During this study, the instrument was operated at a drift tube
166 pressure of 3 mbar, drift tube temperature of 120 °C, and drift tube voltage of 600V, resulting in an operating E/N
167 ratio of ~ 120 Td (1 Td = 10⁻¹⁷ V cm⁻²). These operational instrumental settings are also summarized in Table S1.
168 Ambient air was sampled continuously from the rooftop (~35m A.G.L) through a Teflon inlet line that was
169 protected with a Teflon membrane particle filter (0.2 µm pore size, 47 mm diameter) to ensure that dust and debris
170 did not enter the sampling inlet. The part of the inlet line that was indoors was well-insulated inside a black hose
171 and heated to 80 °C. The instrument background was acquired regularly (typically every 30 min for 5 min), by
172 sampling VOC-free zero air. VOC-free zero air was produced by passing air through an activated charcoal
173 scrubber (Supelpure HC, Supelco, Bellefonte, USA) and a VOC scrubber catalyst (Platinum wool) maintained
174 at 370 °C. Mass spectra covering the m/z 15 to m/z 450 range were obtained at 1 Hz frequency. An internal
175 standard comprising 1,3-di-iodobenzene (C₆H₃I₂⁺) detected at m/z 330.848 and its fragment ion [C₆H₅I⁺] detected
176 at m/z 204.943 were constantly injected to ensure accurate mass axis calibration, so that any drifts in the mass
177 scale were corrected providing for accurate peak detection. Primary data acquisition of mass spectra was
178 accomplished using the IoniTOF software (version 4.2; IONICON Analytik Ges.m.b.H., 6020 Innsbruck, Austria).
179 This software allows the user to define and perform measurements and displays the measured data in real-time.
180 All the settings related to PTR (Proton Transfer Reaction), TPS (TOF power supply), MPV (Multi-port-valve),
181 and MCP (Multi-channel plate) can be controlled and optimized using this control software. The raw mass spectra
182 and relevant instrumental metadata are stored in HDF5 format. These spectra were further processed using the
183 Ionicon Data Analytik (IDA version 2.2.0.4; Ionicon Analytik GmbH, Innsbruck, Austria) software that has the
184 functionalities for peak search, peak fits and preliminary mass assignments and identification of a broad spectrum
185 of organic compounds. The IDA software employs an automated peak detection routine guided by user-defined
186 sensitivity levels for peak detection, peak fit, and shape. The software then uses chemical composition information
187 based on the exact masses and isotopic patterns and calculates a specific proton transfer rate constant (k-rate)
188 based on the polarizability and dipole moment for the peaks with an assigned chemical formula, instead of using
189 a generic value as was done in previous PTR-TOF-MS measurements in Delhi (Tripathi et al., 2022). We manually
190 checked the values also with the compilation of k rates reported by Pagonis et al., (2019) as an additional check.
191 The user has possibility to define a window for mass accuracy (e.g. 30 ppm). Within this defined range and
192 accuracy window, the software identifies all possible chemical compositions and molecular formulae and
193 calculates the corresponding isotope patterns. These patterns are then compared to find the best-fit chemical
194 composition. The process is carried out iteratively, starting with the lower m/z values, according to the method
195 described in the study by Stark et al., (2015).
196 In this study, a total of 1126 peaks were detected in the raw measured ambient mass spectra. After further
197 additional quality control and assurance steps performed manually as detailed in the Section 3.0, 111 compounds
198 present in ambient air for which the molecular formula could be confirmed unambiguously are reported and for
199 which isotopologues due to molecules of different chemical composition could be ruled out completely, were
200 further analysed in this work. Fig S1 provides an example of visualization of mass spectra and peak assignment
201 using the IDA software which also illustrate the high mass resolving power of the PTR-ToF-MS 10K, that enables
202 separation of ion signals that differ by less than 0.04 Th. A certified VOC calibration gas mixture (Societa Italiana
203 Acetilene E Derviat; S.I.A.D. S.p.A., Italy) containing 11 hydrocarbons at ~100 ppb, namely methanol,
204 acetonitrile, acetone, isoprene, benzene, toluene, xylene, trimethylbenzene, and dichlorobenzene and

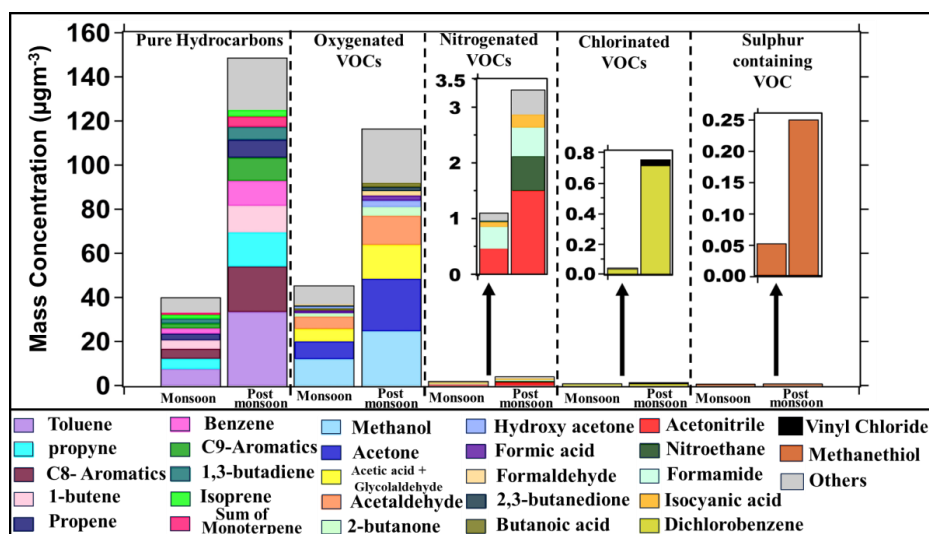


205 trichlorobenzene was used during the field deployment for measuring the transmission and sensitivity of
 206 compounds covering the mass range ($m/z=33$ to $m/z = 181$). The instrument was calibrated a total of 8 times
 207 during the study period: 21.07.2022 after first installation, 26.09.2022, 21.10.2022, 26.10.2022, 5.11.2022,
 208 11.11.2022, 16.11.2022 and 30.11.2022. Results were reproducible across all experiments and a transmission
 209 curve obtained from one of the calibration experiments is shown in Fig. S2. Measured transmission further allowed
 210 for more accurate quantification by accounting for correction of the mass-dependent detection efficiency of the
 211 system. Equation S1 (de Gouw et al., 2007) was then used to convert the measured ion signals to mixing ratios.
 212 The linearity for compounds available in the VOC standard were also checked independently and was above $r \geq$
 213 0.9 as illustrated in Fig S3 for the tested range of ~ 2 to 8 ppb. The background corrected concentrations of all the
 214 detected m/z were exported from IDA in .csv format and further analysis of the dataset was carried out using
 215 IGOR Pro software (version 6.37; WaveMetrics, Inc.).
 216 Carbon monoxide (CO) was measured using IR filter correlation-based spectroscopy air quality analyzer (Thermo
 217 Fischer Scientific 48i) while ozone was measured using UV absorption photometry (Model 49i; Thermo Fischer
 218 Scientific, Franklin, USA). The overall uncertainty of the measurements was less than 6%. Details concerning
 219 characterization of the instrument including calibration and data QA/QC protocols have been comprehensively
 220 described in our previous works (Chandra and Sinha, 2016; Kumar et al., 2016; Sinha et al., 2014).

221 3. Result and Discussion:

222 2.1: Analyses of ambient mass spectra and mass concentration contributions of VOC chemical classes

223



224

225 **Figure 2: Histogram of 111 compounds class-wise, namely Pure Hydrocarbons, Oxygenated VOCs (OVOCs),**
 226 **Nitrogen-containing VOCs (NVOCs), Chlorine-containing VOCs (ClVOCs), and sulphur-containing VOC (SVOC) in**
 227 **both monsoon and post-monsoon periods.**

228



229 A total of 1126 peaks were detected in the raw mass spectra. To identify the ambient compounds of relevance in
230 Delhi from these detected peaks, the following additional manual quality control checks were undertaken. First,
231 peaks attributed to non-ambient compounds such as the impurity ions (e.g. NO^+), water cluster ion peaks, and
232 peaks associated with internal standards were excluded resulting in 1025 peaks for further consideration. Next,
233 the diel profiles and detection limits of these 1025 ion peaks were perused. Only 319 ions out of the 1025 ions
234 showed some diurnal variability and had values above the detection limit after accounting for the respective
235 instrumental background. Next, we verified the presence and expected theoretical magnitude of the shoulder
236 isotopic peaks based on the natural isotopic distribution abundance of the elemental composition of the ion. This
237 was feasible for all m/z except the C1 oxygen containing analyte ions, where the shoulder peak was below
238 detection limit. The preceding QA/QC resulted in an unambiguous assignment for 111 of the 319 ions. Note that
239 these 111 explained 86% of the total mass concentration (μgm^{-3}) observed due to the 319 detected peaks when
240 accounting for the isotopic peaks as well. Table S2 lists the ion m/z and molecular formula of the corresponding
241 compound, along with the averaged mixing ratios observed in each case during the monsoon and post-monsoon
242 season. Additionally, the characteristic ambient diel profile classification as one of the following: unimodal with
243 daytime peak for biogenic/ evaporative/ photochemical source emitted compounds, bimodal with morning and
244 evening peaks for compounds driven by primary emissions (e.g. toluene) and trimodal which were hybrid of the
245 former two, are also provided for each species. Compound names were attributed to specific ions using
246 assignments reported at that m/z in the compiled peer-reviewed PTR-MS mass libraries published by Yáñez-
247 Serrano et al., (2021) and Pagonis et al., (2019) as well as previously published pioneering reports by Stockwell
248 et al. (2015), Sarkar et al. (2016), Yuan et al. (2017) and Hatch et al. (2017). For the same molecular formula,
249 several isomeric compounds with differing chemical structures are possible, with the number of possibilities
250 increasing enormously with an increase in the number of atoms that make up the molecule. Nonetheless in the
251 interest of stimulating interest and further investigation as many have been previously rarely reported or are being
252 reported for the first time in ambient air, we have made bold to provide one of the many possible chemical
253 structures in the Table S2. We do caution that the chemical structure provided by no means even constitutes a best
254 guess estimate but nonetheless would be appealing to chemists and provoke further detailed reporting rather than
255 just the molecular formula.

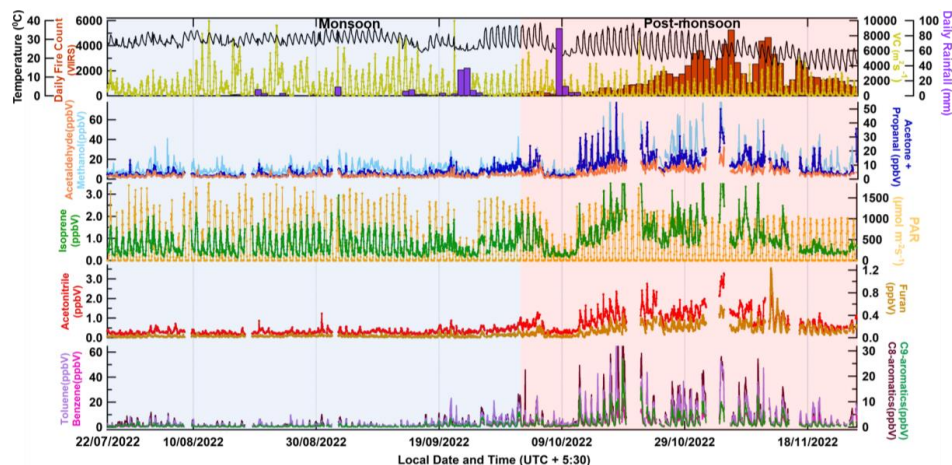
256 A summary of the distribution of the 111 compounds in terms of chemical classes showing their averaged
257 measured ambient mass concentration (μgm^{-3}) contributions is shown in Fig. 2 for the monsoon (22nd July – 30th
258 September 2022) and post-monsoon seasons (1 October- 26 November 2022). Out of the 111 compounds, 42 were
259 pure hydrocarbons made up only of carbon and hydrogen atoms, 56 were oxygenated volatile organic compounds
260 (OVOCs) made up of only carbon, hydrogen and oxygen, 10 contained nitrogen (NVOCs), 2 contained chlorine
261 (ClVOCs), and 1 contained sulphur (SVOC). The average total mass concentration of the same set of pure
262 hydrocarbons during post-monsoon season was 3.7 times greater than in monsoon season ($40 \mu\text{gm}^{-3}$ vs $148 \mu\text{gm}^{-3}$)
263 while the average total mass concentration of OVOCs during post-monsoon was 2.6 times greater than the
264 monsoon season values ($44 \mu\text{gm}^{-3}$ vs $116 \mu\text{gm}^{-3}$). Pure hydrocarbons and OVOCs contributed similarly to the
265 mass concentrations in monsoon season but during the post-monsoon season, the contribution of pure
266 hydrocarbons was significantly higher than that of OVOCs, due to an increase in primary emissions of these
267 compounds. The average mass concentration of NVOCs during post-monsoon was thrice as high relative to the
268 monsoon season ($1 \mu\text{gm}^{-3}$ and $3 \mu\text{gm}^{-3}$). For the chlorine containing VOCs the post-monsoon, concentrations were



269 20 times higher, though in absolute magnitude, the values were low ($1 \mu\text{gm}^{-3}$). The average mass concentration of
270 sulphur containing VOCs during post-monsoon was 4 times higher, but again absolute values were low ($0.2 \mu\text{gm}^{-3}$).
271 ³). The top 10 pure hydrocarbon compounds by mass concentration ranking were toluene, sum of C8-aromatics
272 (xylene and ethylbenzene isomers), propyne, 1-butene, benzene, sum of C9-aromatics (trimethyl benzene
273 isomers), propene, sum of monoterpenes, isoprene and 1,3 butadiene and contributed to 84% of the total mass
274 concentration due to pure hydrocarbons during both the monsoon and post-monsoon seasons, respectively, while
275 the top 20 contributed to 95% and 96% of the total mass concentration in monsoon and post-monsoon,
276 respectively. The top 10 OVOCs: methanol, acetone, acetic acid+ glycolaldehyde, acetaldehyde, hydroxyl-
277 acetone, formaldehyde, 2-butanone, 2,3-butanedione, formic acid, butanoic acid collectively contributed to 84%
278 and 79% of the total mass concentration due to all OVOCs in monsoon and post-monsoon, respectively, while the
279 top 20 contributed to 93% and 90% of the total mass concentration in monsoon and post-monsoon, respectively.
280 The top 4 NVOCs namely acetonitrile, nitroethane, formamide and isocyanic acid contributed to 92% and 91%
281 of the total mass concentration in monsoon and post-monsoon, respectively. Out of 2 identified chlorine containing
282 VOCs, dichlorobenzene ($\text{C}_6\text{H}_4\text{Cl}_2$) was found to be the major contributor contributing 87% and 95% of the total
283 mass concentration in monsoon and post-monsoon, respectively. The only sulphur containing VOC was
284 methanethiol [CH_4S] detected at its protonated ion m/z 49.007 and confirmed by the shoulder isotopic peak.
285 Overall, there was an increase in the mass concentration of all the classes of VOCs from monsoon to post-
286 monsoon. This increase in mass concentration could be attributed to increased emissions from sources that get
287 active in post-monsoon, such as regional post-harvest paddy residue burning, increased open waste burning as
288 well reduced wet scavenging and ventilation coefficient compared to the monsoon season. We examine these in
289 more detail in the next sections.

290 2.2: Time series of VOC tracers during the “clean” monsoon and “polluted post-monsoon” seasons in Delhi

291



292

293 **Figure 3: Time series of hourly data for meteorological parameters like temperature (C) and ventilation coefficient**
294 **(m^2s^{-1}), daily rainfall and daily fire counts (top panel); hourly mixing ratios of methanol, acetaldehyde, and the sum**
295 **of acetone and propanol (second panel from top); isoprene and PAR ($\mu\text{molm}^{-2}\text{s}^{-1}$) (third panel); acetonitrile and furan**
296 **(second panel from bottom); and benzene, toluene and the sum of C8 – aromatics (xylene and ethylbenzene isomers)**



297 **and the sum of C9 – aromatics (isomers of trimethyl benzene and propyl benzene) (bottom panel). The blue and red**
298 **shaded regions represent the monsoon and post-monsoon periods, respectively.**

299

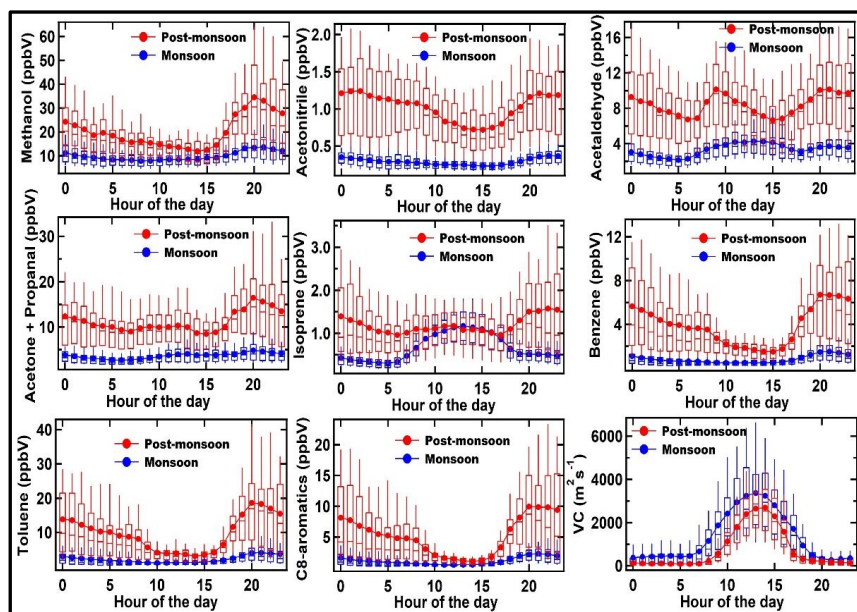
300 Figure 3 shows the time series plot of meteorological parameters and the mixing ratios of some key VOC tracer
301 molecules during monsoon (22nd July – 30th September 2022, blue-shaded region) and post-monsoon (1st October
302 – 26th November 2022, red-shaded region). The top panel shows the ambient Temperature (⁰C), daily VIIRS fire
303 counts on the left side of the top panel and ventilation coefficient (m²s⁻¹), and daily rainfall (mm) on the right side
304 of the top panel during the study period (22nd July 2022 – 26th November 2022). A grid (1km × 1km) with latitudes
305 between 21⁰N and 32⁰N and longitudes between 78⁰E and 88⁰E was considered for extracting the fire count data.
306 The second panel from the top represents the time series of mixing ratios of OVOCs which can be formed photo-
307 chemically as well as be emitted from anthropogenic sources, namely methanol, acetaldehyde, and the sum of
308 acetone and propanol; the third panel shows the mixing ratio of isoprene (a daytime biogenic chemical tracer, pure
309 hydrocarbon) and photosynthetic active radiation (PAR) (μmol photons m⁻² s⁻¹), and the fourth panel shows the
310 mixing ratio of acetonitrile (a biomass burning chemical tracer) and furan (a combustion chemical tracer). The
311 bottom panel shows the mixing ratios of benzene, toluene, the sum of C8–aromatics (xylene and ethylbenzene
312 isomers), and the sum of C9–aromatics (trimethylbenzene and propyl benzene isomers). These are some of the
313 most abundant VOCs typically present in any urban megacity environment, due to their strong emission from
314 traffic and industries in addition to biomass burning (Sarkar et al., 2016; Sinha et al., 2014; Chandra et al., 2016;
315 Singh et al., 2023; Dolgorouky et al., 2012; Yoshino et al; 2012; Langford et al., 2010). We note that all the
316 meteorological conditions and fire activity and VOC levels changed significantly between the much “cleaner”
317 monsoon season and “highly polluted” post-monsoon season at the same site. While the average temperature
318 during monsoon season was 29.5±2.8 °C, in the post-monsoon season this changed to 24.8±5.2 °C, while the
319 average ventilation co-efficient was 1.7 times higher during monsoon season relative to the post-monsoon season.
320 Except for the period impacted by heavy rainfall due to western disturbance weather (8th Oct – 10th Oct 2022),
321 the average mixing ratios for all compounds were considerably higher in the post-monsoon season relative to the
322 monsoon season even after accounting for the ventilation coefficient reduction with all the aromatics compounds
323 like benzene, toluene, sum of C8 and C9 aromatics, all 4.5 times higher and furan more than 5 times higher and
324 acetonitrile, acetone more than 3 times higher and methanol and acetaldehyde 2 times higher. Even isoprene was
325 1.7 times higher but its night time mixing ratios were higher than daytime mixing ratios during post-monsoon
326 season relative to the monsoon season. The increases clearly exceed what can be accounted for only by the reduced
327 ventilation co-efficient (seasonality) and suggests an increase in anthropogenic combustion related sources in
328 particular from open biomass burning fire sources, which we investigate in more detail in the subsequent sections.

329 **2.3: Analyses of the diel profiles during the “clean” monsoon and “polluted post-monsoon” seasons in Delhi** 330 **for discerning major drivers of their ambient values**

331 Figure 4 shows the box and whiskers plot of the same key VOCs like methanol, acetonitrile, acetaldehyde, acetone
332 and propanal, furan, isoprene, benzene, toluene and C8 - aromatics for monsoon (derived from ~ 1704 data points,
333 blue markers) and post-monsoon (derived from ~1368 data points, red markers) against the hour of the day (the
334 horizontal axis represents the start time of the corresponding hourly bin). This more clearly brings out the season-
335 wise diel variation of the compounds and in turn throws light on the emission characteristics and how they vary
336 for the same compound between seasons. Both in the monsoon and post-monsoon season, methanol mixing ratios



337 seem to be driven by primary emission sources and correlate very well with toluene, a tracer for traffic emissions,
338 with highest increases in the evening hours (17:00 to 20:00 L.T.). Globally the main source of methanol is
339 vegetation but in a megacity like Delhi that possesses more than 150000 CNG vehicles and light duty diesel
340 vehicles, it appears that traffic (see Fig 1 of (Hakkim et al., 2021) emitted methanol controls its ambient
341 abundance. Similarly, traffic emissions seem to be a major contributor for acetaldehyde, acetone, sum of C8-
342 aromatics and benzene in the morning and evening hours. Average ambient mixing ratios of acetonitrile, a
343 compound emitted significantly from biomass burning (Holzinger et al., 1999), were below 0.5 ppb in the
344 monsoon for all hours, with only slight increase at night, but during post-monsoon season, for all hours the values
345 doubled to 1 ppb, with strong increases in the early evening and night time hours. This tendency was mirrored in
346 all the other compounds including isoprene. The diel profile of isoprene and acetaldehyde were the only ones
347 which showed daytime maxima during the monsoon season. This shows that during the monsoon season, the
348 biogenic sources of isoprene majorly drive its ambient mixing ratios, whereas acetaldehyde ambient mixing ratios
349 are controlled by photochemical production of the compound in the monsoon season. Under the high NO_x
350 conditions prevalent in a megacity like Delhi, photo-oxidation of n-butane, propene, ethane and propane could be
351 a large photochemical source of acetaldehyde (Millet et al., 2010).
352



353
354 **Figure 4: Box and whisker plots showing average, median, and variability (10th, 25th, 75th and 90th percentile)**
355 **for some major VOCs and the ventilation coefficients (m^2s^{-1}) during monsoon and post-monsoon periods. The blue and**
356 **red markers represent the monsoon and post-monsoon periods, respectively.**

358 Benzene which is human carcinogen is the only VOC for which there is a national ambient air quality standard (5
359 $\mu\text{g m}^{-3}$ equivalent to ~ 1.6 ppb at 298 K) in India. Average mixing ratios in the post-monsoon season (Fig 4) were
360 always above this value no matter what hour of the day, and the seasonal average was twice as high as this value
361 (~ 4 ppb). The increased biomass burning in post-monsoon season controlled the abundance of benzene,



362 acetaldehyde and acetone and isoprene during this period, due to strong emissions from both biomass burning and
363 traffic. The typical atmospheric lifetimes of all these compounds spans from few hours (e.g. isoprene) to several
364 days (e.g. benzene and methanol) and several months in the case of acetonitrile. As potent precursors of secondary
365 organic aerosol, the aromatic compounds would also enhance secondary organic aerosol pollutant formation
366 during the polluted post-monsoon season. When compared with the first PTR-MS measurements of these
367 compounds reported from wintertime Delhi (see Fig 2 of Hakkim et al., 2019), the average levels of these
368 compounds for the post-monsoon season (Table S2) are lower or comparable, but still significantly higher than
369 what has been reported for other major cities of the world like Tokyo, Paris, Kathmandu, Beijing, London (Yoshino
370 et al., 2012; Dolgorouky et al., 2012; Sarkar et al., 2016; Li et al., 2019; Langford et al., 2010). The monsoon
371 levels on the other hand were comparable to many of the other megacities.

372 As the monsoon season is characterized by favourable meteorological conditions for wet scavenging and dispersal
373 due to higher ventilation co-efficient, as well as significantly lower open biomass burning due to wet and warm
374 conditions, the monsoon levels can be considered as baseline values for the ambient levels of these compounds
375 (except isoprene and acetaldehyde) in Delhi, which are driven mainly by year-round traffic and industrial sources
376 in Delhi. In monsoon for isoprene, the major driver are biogenic sources whereas for acetaldehyde the major driver
377 is photochemistry, a finding that is similar to what has reported from another site in the Indo-Gangetic Plain
378 previously (Mishra and Sinha, 2020).

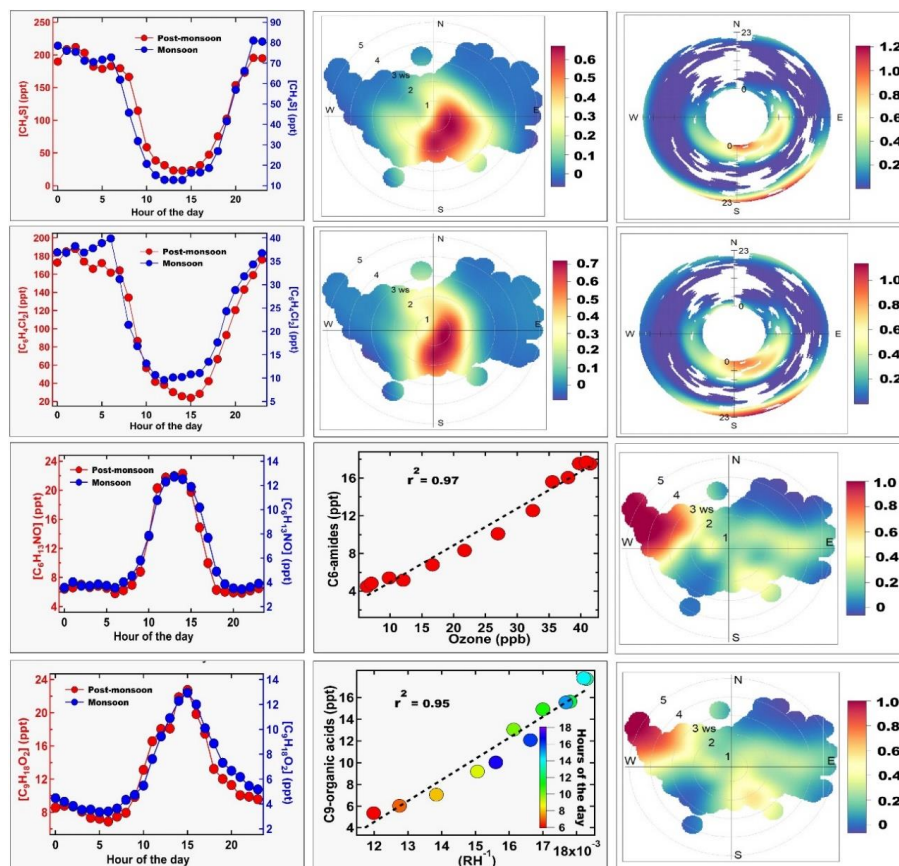
379 **2.4: Discovery of methanethiol (CH_3SH), dichlorobenzenes ($\text{C}_6\text{H}_4\text{Cl}_2$), and C6-amides ($\text{C}_6\text{H}_{13}\text{NO}_2$) and C9- 380 **organic acids ($\text{C}_9\text{H}_{18}\text{O}_2$) in ambient Delhi air****

381 Figure 5 shows the average diel profile of four compounds present in both monsoon and post-monsoon periods
382 that have to our knowledge never been reported from Delhi or any site in South Asia and only rarely been reported
383 in the gas phase in any atmospheric environment in the world. Except for methanethiol detected at m/z 49.007
384 (also called methyl mercaptan), all the other compounds namely dichlorobenzene ($\text{C}_6\text{H}_4\text{Cl}_2$) detected at m/z
385 146.977, C6-amides like hexanamide ($\text{C}_6\text{H}_{13}\text{NO}_2$) and its isomers detected at m/z 116.108 and C9- carboxylic
386 acid/ester such as nonanoic acid ($\text{C}_9\text{H}_{18}\text{O}_2$) and its isomers detected at m/z 159.14, are all intermediate volatility
387 range organic compounds. These could be detected so well, mainly due to our extended volatility range mass
388 spectrometer design and high sensitivity due to ion booster and hexapole guide of the PTR-TOF-MS 10 K system,
389 which has been missing in previous PTR-TOF-MS deployments in India. The presence of such reactive organic
390 sulphur, chlorine and nitrogen containing compounds in the gas phase was surprising and provides new insights
391 concerning the chemical composition and secondary chemistry occurring in air, during the extremely high
392 pollution events. Below we examine the sources and chemistry of these compounds in further detail.

393 The diel profiles of both methanethiol and dichlorobenzene in both the monsoon and post-monsoon seasons were
394 similar (bimodal with afternoon minima), and controlled by the ventilation coefficient diel variability (see Fig. 4),
395 and in fact even the difference in their average magnitudes (50 ppt Vs 130 ppt for CH_3SH and 25 ppt Vs 100 ppt
396 for dichlorobenzene between monsoon and post-monsoon seasons), can largely be explained by the reduction in
397 ventilation co-efficient (~2 reduction). Further, the conditional probability wind rose plots for both compounds
398 shows that the high values come from the same wind sector upwind of the site spanning north-east to south during
399 early morning and evening hours, which is actually where a variety of industrial sources are located. Previously,
400 Nunes et al., (2005) and Kim et al., (2006) have reported methanethiol from petrochemical industries and landfills



401 in Brazil and Korea, respectively. Toda et al., (2010) reported high (tens of ppb) methanethiol mixing ratios from
402 a pulp and paper mill industry in Russia.
403



404
405 **Figure 5: Average diurnal profile of methanethiol, isomers of dichlorobenzene, C6-amides, and C9- organic acid in**
406 **the left panel for both monsoon (blue marker) and post-monsoon (red marker) periods. The second panel shows the**
407 **wind rose plot of methanethiol and isomers of dichlorobenzene, plot of C6-amide vs ozone and C9-organic acid vs**
408 **RH⁻¹ colour coded by the hour of the day. The third panel shows the polar annulus plot of methanethiol, isomers of**
409 **dichlorobenzene and wind rose plot of C6-amides and C9-organic acid.**

410
411 Both compounds are also used in the deodorant and pesticide products as reagents and although large scale
412 pesticide manufacturing facilities were shifted out of Delhi, there are still units that sell and distribute these
413 products in those areas, from which fugitive emissions are likely happening. Methanethiol is further used as a
414 precursor in methionine production, an essential amino acid used in manufacture of pesticides, and fragrances
415 industry uses methanethiol for its distinct sulphur-like aroma, contributing to the creation of savory flavors and
416 unique fragrances. In the Delhi environment, a combination of such industries, in particular paper and pulp
417 industries, are likely candidate sources. Methanethiol is an extremely reactive molecule reacting primarily with
418 the hydroxyl radical (OH) during daytime with an estimated lifetime of 4.3 h (Wine et al., 1981). Its photo-
419 oxidation in daytime with hydroxyl radicals produces sulphur dioxide, methanesulfonic acid, dimethyl disulphide



420 and sulphuric acid (Kadota and Ishida et al., 1972; Hatakeyama et al., 1983), all of which play key roles in aerosol
421 formation pathways. Further it can also react with nitrate radicals (Berreshiem et al., 1995) and participate in
422 night-time chemistry. More recently Reed et. al. (2020) reported that presence of even trace amounts of such
423 compounds can significantly enhance organic aerosol mass and particle effective density, and such organosulfur
424 compounds provide evidence that sulphur and carbon chemistry coupling can impact the organic haze and
425 atmospheric sulphur chemistry in planetary atmospheres, and to our knowledge the present study presents the first
426 evidence from a polluted megacity supporting the hypothesis (Reed et al., 2020). Wine et al. (1981) had further
427 predicted that the very rapid rate at which methanethiol reacts with OH would result in low steady-state
428 concentrations in ambient air, even though reasonably large-scale sources may exist. Our findings are also
429 consistent with this and though the ambient levels detected were few 100 ppt, the fact is that the global
430 methanethiol sales was ~9 billion US dollars in 2023 and is expected to further grow (Coherent market insight,
431 last access: 19 January 2024).

432 Several recent studies have reported high chloride in sub-micron aerosol of Delhi (Gani et al., 2020; Acharja et
433 al., 2023; Pawar et al., 2023). Dichlorobenzene is an intermediate range volatile organic compound (IVOC) which
434 can partition between gas and aerosol phase. However, till date no gaseous IVOC chlorinated organic compound
435 have been reported in ambient air from India. p-dichlorobenzene (PDCB) also called 1, 4-dichlorobenzene, one
436 of the dichlorobenzene isomers is known for its use as a pest repellent and deodorant in indoor environments. 1,4-
437 dichlorobenzene in outdoor air in various locations of North America and Europe ranged from 30 ppt to 830 ppt
438 (Chin et al., 2013). It is emitted only from anthropogenic sources as there are no known natural sources. Its
439 emission sources include consumer and commercial products containing PDCB, waste sites, and manufacturing
440 facilities for flavour and as insect repellent products (ATSDR. 2006). Its atmospheric lifetime is estimated to be
441 21–45 days (Mackay et al., 1997). It has been reported as a precursor of secondary organic aerosol in indoor
442 conditions (Komae et al., 2020). Due to its long lifetime, dichlorobenzene can be transported to upper regions of
443 the atmosphere where some release of some reactive chlorine through photolysis can occur, but this is not likely
444 to be of large consequence. Instead, reaction with hydroxyl radicals would convert it more readily to phenolic
445 compounds that would readily partition to aqueous aerosol phase and also undergo nitration to form nitrophenolics
446 (Hu et al., 2021), which are a component of brown carbon (Lin et al. 2015, 2017).

447 In contrast, the diel profile of the average mixing ratios of $C_6H_{13}NO$ (Fig. 5), likely hexanamide or isomers of C6-
448 amides measured at m/z 116.108, was similar in both monsoon and post-monsoon season and characteristic of a
449 compound with a purely photochemical source with no evening time peaks even during the enhanced biomass
450 burning in post-monsoon season. As observed for several other compounds in this study, the difference in
451 magnitude between both seasons (peak value 22 ppt in post-monsoon season vs 12 ppt in monsoon season) could
452 be accounted for almost completely by the reduced ventilation co-efficient in post-monsoon season (factor of ~2).
453 The presence of photochemically formed formamide and acetamide from OH oxidation of alkyl amine precursors
454 has been previously reported (Chandra et al., 2016; Kumar et al., 2018), from another site in the Indo-Gangetic
455 Plain which experiences strong agricultural waste burning. In the literature we could only find only one report for
456 presence of C6 amides in the ambient air in the gas phase (Yao et al., 2016), who reported ~14 ppt in summertime
457 air of Shanghai using an ethanol reagent ion CIMS, the source of which was both industrial and photochemical
458 origin. However, to our knowledge this is the first study world-wide to detect and report only photo-chemically
459 formed C6-amides in the gas phase. C6-amides are IVOCs, which can easily partition to aerosol phase depending



460 on environmental conditions and also act as a new source of reactive organic nitrogen to the atmospheric
461 environment. We found the highest values in air masses arriving in the afternoon from the north-west direction at
462 high wind speeds (see Fig 5) during the post-monsoon season, which indicated that paddy stubble burning
463 emissions of amines (Kumar et al., 2018) were its likely precursors. The mechanism of amide formation through
464 photochemical reactions has been elucidated in several previous laboratory studies (Bunkan et al., 2016, Barnes
465 et al., 2010; Nielsen et al., 2012; Borduas et al., 2015). When correlated with daytime ozone hourly mixing ratios,
466 the very high correlation ($r^2 > 0.97$), confirmed its purely photochemical origin. Being an amide, further gas phase
467 oxidation products are likely to result in organic acids or condensation on existing aerosol particles which could
468 add to the reactive organic nitrogen in aerosol phase and neutralize acidity just like ammonia, as ammonium ion
469 is formed from hydrolysis of amides (Yao et al., 2016). However, the exact role of these amides in nucleation and
470 aerosol chemistry will warrant further investigations.

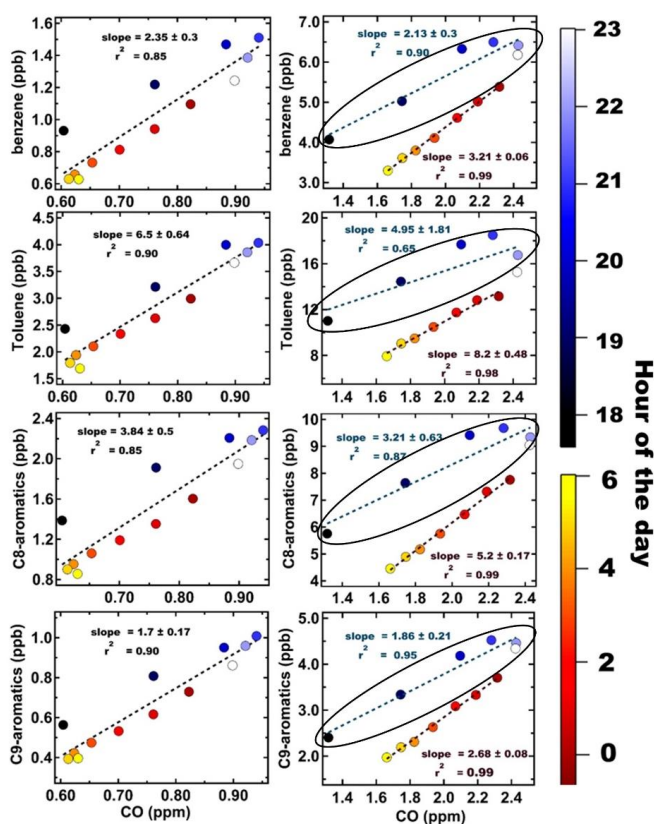
471 Finally, the last row of Fig. 5 shows the average mixing ratios of the compound with molecular formula $C_9H_{18}O_2$
472 which is likely due to isomers of C9- carboxylic acids (e.g. nonanoic acid), although one cannot rule out
473 contributions from isomers of esters such as methyl octanoate or 2-methylbutyl isobutyrate also detected at m/z
474 159.14. Although here also there is a daytime peak, the timing of the peak is much later in the day (15:00 local
475 time). The peak hourly values reached 24 ppt in post-monsoon season. It showed high correlation ($r^2 > 0.95$) with
476 the inverse of the ambient daytime relative humidity indicating that it partitions back and forth between the gas
477 phase and aerosol phase depending on the environmental conditions of temperature and RH. n-alkanoic acids in
478 general and nonanoic acid in particular have long been reported as major organic acids present in biomass burning
479 emitted organic aerosol (Oros et al., 2006; Fang et al., 1999). The corresponding wind rose plot (Fig. 5) shows
480 that the highest values were in air masses arriving at high wind speeds in the afternoon from the north-west during
481 post-monsoon season, which is a major source region of biomass burning emitted organic aerosols. It is also
482 possible that photochemical oxidation through ozonolysis of precursors and hydroxyl radical initiated oxidation
483 can form such carboxylic acids as an advanced oxidation product (Kawamura et al., 2013). In both cases, biomass
484 burning emissions and evaporation from aerosol phase, appear to be the major source of this compound.
485 Carboxylic acids in the aerosol phase would serve to neutralize some of the excess ammonia in the atmospheric
486 environment of the Indo-Gangetic Plain (Acharja et al., 2022) and would be important for night-time aerosol
487 chemistry in Delhi.

488 **2.5: Comparison of ambient mixing ratios and VOC/CO emission ratios for aromatic VOCs in Delhi with** 489 **some megacities of Asia, Europe and North America**

490 Aromatic compounds are among the most important class of compounds in urban environments due to their direct
491 health effects (e.g. benzene is a human carcinogen), and reactivity as ozone and secondary organic aerosol
492 precursors. Therefore, these compounds have been widely investigated in many cities and information concerning
493 their ambient levels and emission ratios to carbon monoxide is often used for assessing similarities and differences
494 in the sources of these compounds in varied urban environments (Warneke et al., 2007; Borbon et al., 2013). In
495 Figure 6, we show the emission ratios (ER) derived for benzene, toluene and the sum of C8 and C9 aromatic
496 compounds (VOC / CO ppb/ppm) using night-time monsoon (left panel) and post monsoon (right panel)
497 measurements made in Delhi. The method is based on a linear regression fit to determine the slope of the night-
498 time scatterplot data (from 20:00 to 06:00 L.T.) between a VOC (ppb) and CO (ppm) (de Gouw et al., 2017,
499 Borbon et al., 2013). Using night-time hourly data (18:00 to 06:00 L.T.) provides the advantage of minimizing



500 complications due to daytime oxidative losses of the compounds. It can be noted from Fig. 6, that during the
 501 monsoon season, the spread of values is much less and a single line fits the slope. For post-monsoon season on
 502 the other hand, there appears to be an additional source that becomes important after the evening traffic rush hours
 503 are over and both these sources have different characteristic emission ratios (with different linear fits and slopes)
 504 with respect to CO. This suggests that in addition to traffic exhaust emissions which are a year-round active source,
 505 in the post-monsoon season other biomass combustion/ industrial sources also play an important role in governing
 506 the budgets of these aromatic compounds.



507
 508 **Figure 6: Emission ratios (VOC (ppb)/CO (ppm)) of benzene, toluene, C8 aromatics and C9 aromatics for both**
 509 **monsoon (left panel) and post monsoon (right panel) periods respectively. The data points for each period are colour**
 510 **coded with the hour of the day (18:00 L.T to 06:00 L.T).**

511
 512 Table 1 provides a comparison of the ambient mixing ratios and emission ratios that have been reported in some
 513 other major megacities of Asia, Europe and North America for these compounds. Although, the year of
 514 measurements and seasons are not the same, nonetheless such comparison helps put the 2022 levels of these
 515 compounds in Delhi in a global context.

516
 517 **Table 1: Comparative summary of the average mixing ratio (ppb) and Emission Ratios of VOC/ CO (ppb/ppm) of**
 518 **Delhi (in parentheses) with other megacities of Asia, Europe and North America**
 519



VOC	Delhi*	Langzhou Valley ^l	Sao Paulo ²	London ³	Los Angeles ^{4(a)}	Paris ^{5(a)}	Mexico City ^{6(b)}	New York ^{4(c)}	Beijing ^{7(d)}	Lahore ⁸
Benzene	2.02 (2.65)	0.54 (1.37)	0.67 (1.03)	0.31 (1.59)	0.48 (1.30)	0.38 (1.07)	0.80 (1.21)	0.74 (1.09)	1.79 (1.24)	28.20 (5.08)
Toluene	5.15 (7.03)	0.72 (1.41)	2.11 (3.1)	0.60 (3.09)	1.38 (3.18)	1.40 (12.30)	3.10 (4.20)	0.19 (3.79)	1.98 (2.41)	32.40 (6.67)
Sum of C8 aromatics	2.74 (4.20)	0.61 (1.42)	1.52 (2.15)	0.63 (3.69)	1.03 (2.45)	1.30 (4.75)	1.10 (4.30)	0.88 (1.11)	2.66 (2.15)	29.40 (6.04)

520 * *This work (2022)* ¹*Zhou et al., (2019)* ²*Brito et al., (2015)* ³*Valach et al., (2014)* ⁴*Baker et al., (2008)*
 521 ^(a)*Borbon et al., (2013)* ⁵*Gros et al., (2011)* ⁶*Garzón et al., (2015)* ⁷*Yang et al., (2019a)* ⁸*Barletta et al.,*
 522 *(2016)* ^(b)*Bon et al., (2011)* ^(c)*Warneke et al., (2007)* ^(d)*Wang et al., (2014)* [†]*Apel et al., (2010)*
 523

524 Except for Lahore, where benzene levels were 10 times higher, benzene levels in Delhi were comparable to Beijing
 525 and about three times higher than those that have been reported from other megacities like Sao Paulo, London,
 526 Los Angeles, Paris, Mexico City and New York. The annual averaged national ambient air quality standard for
 527 benzene is 5 µg m⁻³ in India which is approximately 1.6 ppb at room temperature. Thus, the data suggest that
 528 sources in the investigated period (Monsoon and Post-monsoon season) would contribute to violation of the annual
 529 averaged values. Similarly, toluene and the sum of C8 aromatic compounds (e.g. xylene and ethyl benzene
 530 isomers) were 6 to 10 times higher in Lahore compared to Delhi and more than twice as high relative to the
 531 aforementioned megacities, except for Beijing, where the sum of C8 aromatic compounds were comparable to
 532 Delhi. Overall, this indicates that Delhi has much higher levels of aromatic VOC pollution than many other
 533 megacities. When we peruse the emission ratios that have been reported for these compounds in these other
 534 megacities (shown in parentheses in Table 1), barring few exceptions (e.g. Lahore and Paris), the ERs were
 535 generally much higher in Delhi with an average value of 2.65, as compared to cities like Sao Paulo (Brito et al.,
 536 2015), London (Valach et al., 2014) and Los Angeles and Paris (Borbon et al., 2013), Mexico City (Bon et al.,
 537 2011) and several US cities (Baker et al., 2008). The ER of toluene was highest in Paris (12.3) followed by Delhi.
 538 Overall, the mixing ratios and ERs indicate that the influence of non –traffic sources (e.g. biomass burning and
 539 industries) is more significant in Delhi compared to many other megacities of the world. The companion paper on
 540 source apportionment based on this dataset (Awasthi et al., 2024) will focus more on the quantitative contributions
 541 of the different sources.

542 4. Conclusion

543 This study has provided unprecedented characterization of the VOC chemical composition of ambient air in Delhi
 544 for the clean monsoon and extremely polluted post-monsoon seasons. The total average mass concentration of the
 545 reactive carbon in the form of the 111 VOC species identified unambiguously was ~260 µgm⁻³ and more than 4
 546 times higher during the polluted post-monsoon season mainly due to the impact of large scale open fires and
 547 reduced ventilation relative to the “cleaner” monsoon season. Of the 111, 42 were pure hydrocarbons (CH), 56
 548 were oxygenated volatile organic compounds (OVOCs; CHO), 10 were nitrogen containing compounds (NVOCs;
 549 CHON), 2 were chlorinated volatile organic compounds (ClVOCs), and 1 namely methanethiol, contained
 550 sulphur. The detection of new compounds that have previously not been discovered in Delhi’s air, under both the



551 clean and polluted periods such as methanethiol (CH_3SH), dichlorobenzenes ($\text{C}_6\text{H}_4\text{Cl}_2$), C6-amides ($\text{C}_6\text{H}_{13}\text{NO}_2$)
552 and C9-organic acids ($\text{C}_9\text{H}_{18}\text{O}_2$) in the gas phase was very surprising pointing to both industrial sources of the
553 sulphur and chlorine compounds, photochemical source of the C6-amides and multiphase oxidation and chemical
554 partitioning for the C9-organic acids. To our knowledge this is the first reported study world-wide to detect and
555 observe only photo-chemically formed C6-amides in the gas phase. C6-amides are IVOCs, which can easily
556 partition to aerosol phase depending on environmental conditions and also act as a new source of reactive organic
557 nitrogen to the atmospheric environment.

558 The monsoon season VOC abundances for major compounds were comparable to several other megacities of the
559 world showing that the baseline VOC levels for the city of Delhi due to year-round active sources, helped by
560 favourable meteorological conditions for removal of VOCs through ventilation and wet scavenging, can lead to
561 comparable air quality as observed in other megacities. The VOC levels during the polluted post-monsoon season
562 when severe air pollution events occur leading to shutdowns and curbs, on the other hand were significantly (2-3
563 times) higher. Overall, for many important aromatic VOCs, the levels measured in Delhi were even higher (> 5
564 times) than many other megacities of the world located in Europe and North America.

565 The presence of such a complex mixture of reactant VOCs adds to the air pollutant burden through secondary
566 pollutant formation of aerosols. The reactive gaseous organics were found to rival the high mass concentrations
567 of the main air pollutant in exceedance at this time, namely $\text{PM}_{2.5}$ during the extremely polluted periods. While
568 the present study has quantified the molecules in the gas phase that are important for the air chemistry driving the
569 high pollution events in Delhi in unprecedented detail, the implications on secondary pollutant formation will
570 require building up on this new strategic knowledge and further investigations. Moreover, the unique primary
571 observations will yield quantitative source apportionment of particulate matter and VOCs in a companion study
572 (Awasthi et al., 2024), that is being co-submitted to this journal to enrich the scientific insights.

573 All previous VOC studies in the literature from a dynamically growing and changing megacity like Delhi were
574 reported for periods before 2020 (pre-covid) times, using technology that is not as state of the art as the new
575 enhanced volatility VOC quantification technology deployed for the first time in a complex ambient environment
576 of developing world megacity like Delhi. These have resulted in unprecedented new information concerning the
577 speciation, abundance, ambient variability and emission characteristics of several rarely measured/reported VOCs.

578 The significance of the new understanding concerning atmospheric composition and chemistry of highly polluted
579 urban atmospheric environments gained from this study, will no doubt be of global relevance as they would aid
580 atmospheric chemistry investigations in many megacities and polluted urban environments of the global south,
581 that are in similar development and growth trajectory as Delhi and experience extreme air pollution and air quality
582 associated challenges, but remain understudied.



583 **Data availability**

584 The VOC, CO and Ozone data presented in this manuscript can be obtained by contacting Prof. Vinayak Sinha

585 **Author Contribution**

586 Sachin Mishra: Data curation, Formal analysis, Investigation, Software, Visualization, Writing – original draft
587 preparation. Vinayak Sinha: Conceptualization, Data curation, Formal analysis, Methodology, Project
588 administration, Software, Supervision, Validation, Writing – review & editing. Haseeb Hakkim: Data curation,
589 Formal analysis, Investigation, Writing – review & editing. Arpit Awasthi : Data curation, Formal analysis,
590 Investigation. Sachin D. Ghude: Writing – review & editing. Vijay Kumar Soni: Writing – review & editing. N.
591 Nigam: resources. Baerbel Sinha: Conceptualization, Data curation, Supervision, Writing – review & editing. M.
592 Rajeevan: Writing – review & editing.

593 **Competing Interests**

594 The authors declare that they have no conflict of interest.

595

596 **Acknowledgment**

597 We acknowledge the financial support given by the Ministry of Earth Sciences (MOES), Government of India, to
598 support the RASAGAM (Realtime Ambient Source Apportionment of Gases and Aerosol for Mitigation) project
599 at IISER Mohali vide grant MOES/16/06/2018-RDEAS Dt. 22.6.2021. S.M acknowledges IISER Mohali for
600 Institute PhD fellowship. AA acknowledges MoE for PMRF PhD fellowship. We thank Dr. R. Mahesh, Dr. Gopal
601 Iyengar, Dr. R. Krishnan (Director, IITM Pune), Prof. Gowrishankar (Director, IISER Mohali), Dr. Mohanty (DG,
602 IMD), Dr. M. Ravichandran (Secretary Ministry of Earth Science) for their encouragement and support. We thank
603 student members of the Atmospheric Chemistry and Emissions (ACE) research group and Aerosol Research
604 Group (ARG) of IISER Mohali and IITM Pune in particular Akash Vispute, Prasanna Lonkar and local scientists
605 of IMD for their logistics and moral support. The authors gratefully acknowledge the NASA/ NOAA Suomi
606 National Polar-orbiting Partnership (Suomi NPP) and NOAA-20 satellites VIIRS fire count data used in this
607 publication. The authors gratefully acknowledge the NOAA Air Resources Laboratory (ARL) for the provision
608 of the HYSPLIT transport and dispersion model used in this publication. We thank Campbell Scientific India Pvt
609 Ltd, Ionicon Analytic GmbH and Mars Bioanalytical for technical assistance rendered by them.

610 **References:**

611 Acharja, P., Ali, K., Ghude, S. D., Sinha, V., Sinha, B., Kulkarni, R., Gultepe, I., and Rajeevan, M. N.: Enhanced
612 secondary aerosol formation driven by excess ammonia during fog episodes in Delhi, India, *Chemosphere* 289,
613 133155, <https://doi.org/10.1016/j.chemosphere.2021.133155>, 2022.
614 Acharja, P., Ghude, S.D., Sinha, B., Barth, M., Govardhan, G., Kulkarni, R., Sinha, V., Kumar, R., Ali, K.,
615 Gultepe, I., Petit, J., and Rajeevan, M.N., Thermodynamical framework for effective mitigation of high aerosol



- 616 loading in the Indo-Gangetic Plain during winter. *Sci Rep* 13, 13667 <https://doi.org/10.1038/s41598-023-40657->
617 [w](https://doi.org/10.1038/s41598-023-40657-w), 2023.
- 618 Apel, E. C., Emmons, L. K., Karl, T., Flocke, F., Hills, A. J., Madronich, S., Lee-Taylor, J., Fried, A., Weibring,
619 P., Walega, J., Richter, D., Tie, X., Mauldin, L., Campos, T., Weinheimer, A., Knapp, D., Sive, B., Kleinman, L.,
620 Springston, S., Zaveri, R., Ortega, J., Voss, P., Blake, D., Baker, A., Warneke, C., Welsh-Bon, D., de Gouw, J.,
621 Zheng, J., Zhang, R., Rudolph, J., Junkermann, W., and Riemer, D. D.: Chemical evolution of volatile organic
622 compounds in the outflow of the Mexico City Metropolitan area, *Atmos. Chem. Phys.*, 10, 2353–2375,
623 <https://doi.org/10.5194/acp-10-2353-2010>, 2010.
- 624 ATSDR.: Toxicological Profile for 1,4-Dichlorobenzene, Atlanta, GA, Agency for Toxic Substances and Disease
625 Registry, U.S. Department of Health and Human Services, 2006.
- 626 Awasthi, A., Sinha, B., Hakkim, H., Mishra, S., Varkrishna, M., Singh, G., Ghude, S. D., Soni, V.K., Nigam, N.,
627 Sinha, V., and Rajeevan M.: Biomass burning sources control ambient particulate matter but traffic and industrial
628 sources control VOCs and secondary pollutant formation during extreme pollution events in Delhi, *Atmos. Chem.*
629 *Phys. Discuss.*, (submitted), 2024.
- 630 Baker, A. K., Beyersdorf, A. J., Doezema, L. A., Katzenstein, A., Meinardi, S., Simpson, I. J., Blake, D. R., and
631 Sherwood Rowland, F.: Measurements of nonmethane hydrocarbons in 28 United States cities, *Atmos. Environ.*,
632 42, 170-182, <https://doi.org/10.1016/j.atmosenv.2007.09.007>, 2008.
- 633 Barletta, B., Simpson, I. J., Blake, N. J., Meinardi, S., Emmons, L. K., Aburizaiza, O. S., Siddique, A., Zeb, J.,
634 Yu, L. E., Khwaja, H. A., Farrukh, M. A., and Blake, D. R.: Characterization of carbon monoxide, methane and
635 nonmethane hydrocarbons in emerging cities of Saudi Arabia and Pakistan and in Singapore, *J. Atmos. Chem.*,
636 11, 2399–2421, <https://doi.org/10.1007/s10874-016-9343-7>, 2016.
- 637 Barnes, I., Solignac, G., Mellouki, A., and Becker, K. H.: Aspects of the atmospheric chemistry of
638 amides, *ChemPhysChem*, 11(18), 3844-3857, <https://doi.org/10.1002/cphc.201000374>, 2010.
- 639 Bikkina, S., Andersson, A., Kirillova, E.N., Holmstrand, H., Tiwari, S., Srivastava A. K., Bisht, D. S., and
640 Gustafsson, O.: Air quality in megacity Delhi affected by countryside biomass burning, *Nat Sustain.*, 2, 200–205.
641 <https://doi.org/10.1038/s41893-019-0219-0>, 2019.
- 642 Berresheim, H., Wine, P.H., and Davis, D.D.: Sulfur in the atmosphere. In: Singh, H.B. (Ed.), *Composition,*
643 *Chemistry, and Climate of the Atmosphere*, Van Nostrand Reinhold, New York, ISBN 0-442-01264-0, pp. 251-
644 307, 1995.
- 645 Bon, D. M., Ulbrich, I. M., de Gouw, J. A., Warneke, C., Kuster, W. C., Alexander, M. L., Baker, A., Beyersdorf,
646 A. J., Blake, D., Fall, R., Jimenez, J. L., Herndon, S. C., Huey, L. G., Knighton, W. B., Ortega, J., Springston, S.,
647 and Vargas, O.: Measurements of volatile organic compounds at a suburban ground site (T1) in Mexico City
648 during the MILAGRO 2006 campaign: measurement comparison, emission ratios, and source attribution, *Atmos.*
649 *Chem. Phys.*, 11, 2399–2421, <https://doi.org/10.5194/acp-11-2399-2011>, 2011.
- 650 Borbon, A., Gilman, JB, Kuster, WC, Grand, N, Chevaillier, S, Colomb, A, Dolgorouky, C, Gros, V, Lopez, M,
651 Sarda-Esteve, R, Holloway, J, Stutz, J, Petetin, H, McKeen, S, Beekmann, M, Warneke, C, Parrish, DD, and de
652 Gouw, JA.: Emission ratios of anthropogenic volatile organic compounds in northern mid-latitude megacities:
653 Observations versus emission inventories in Los Angeles and Paris, *J. Geophys Res.-Atmos.*, 118(4): 2041–2057.
654 <http://dx.doi.org/10.1002/jgrd.50059>, 2013.



- 655 Borduas, N., da Silva, G., Murphy, J. G., and Abbatt, J. P.: Experimental and theoretical understanding of the gas
656 phase oxidation of atmospheric amides with OH radicals: kinetics, products, and mechanisms, *J. Phys. Chem.*
657 *A*, 119(19), 4298-4308, <https://doi.org/10.1021/jp503759f>, 2015.
- 658 Brito, J., Wurm, F., Yanez-Serrano, A. M., de Assuncao, J. V., Godoy, J. M., and Artaxo, P.: Vehicular Emission
659 Ratios of VOCs in a Megacity Impacted by Extensive Ethanol Use: Results of Ambient Measurements in Sao
660 Paulo, Brazil, *Environ. Sci. Technol.*, 49, 11381–11387, <https://doi.org/10.1021/acs.est.5b03281>, 2015.
- 661 Bryant, D. J., Nelson, B. S., Swift, S. J., Budisulistiorini, S. H., Drysdale, W. S., Vaughan, A. R., Newland, M. J.,
662 Hopkins, J. R., Cash, J. M., Langford, B., Nemitz, E., Acton, W. J. F., Hewitt, C. N., Mandal, T., Gurjar, B. R.,
663 Shivani, Gadi, R., Lee, J. D., Rickard, A. R., and Hamilton, J. F.: Biogenic and anthropogenic sources of isoprene
664 and monoterpenes and their secondary organic aerosol in Delhi, India, *Atmos. Chem. Phys.*, 23, 61–83,
665 <https://doi.org/10.5194/acp-23-61-2023>, 2023.
- 666 Bon, D. M., Ulbrich, I. M., de Gouw, J. A., Warneke, C., Kuster, W. C., Alexander, M. L., Baker, A., Beyersdorf,
667 A. J., Blake, D., Fall, R., Jimenez, J. L., Herndon, S. C., Huey, L. G., Knighton, W. B., Ortega, J., Springston, S.,
668 and Vargas, O.: Measurements of volatile organic compounds at a suburban ground site (T1) in Mexico City
669 during the MILAGRO 2006 campaign: measurement comparison, emission ratios, and source attribution, *Atmos.*
670 *Chem. Phys.*, 11, 2399–2421, <https://doi.org/10.5194/acp-11-2399-2011>, 2011.
- 671 Bunkan, A. J. C., Mikoviny, T., Nielsen, C. J., Wisthaler, A., and Zhu, L. (2016): Experimental and theoretical
672 study of the OH-initiated photo-oxidation of formamide, *J. Phys. Chem. A*, 120(8), 1222-1230,
673 <https://doi.org/10.1021/acs.jpca.6b00032>, 2016.
- 674 Cash, J. M., Langford, B., Di Marco, C., Mullinger, N. J., Allan, J., Reyes-Villegas, E., Joshi, R., Heal, M. R.,
675 Acton, W. J. F., Hewitt, C. N., Misztal, P. K., Drysdale, W., Mandal, T. K., Shivani, Gadi, R., Gurjar, B. R., and
676 Nemitz, E.: Seasonal analysis of submicron aerosol in Old Delhi using high-resolution aerosol mass spectrometry:
677 chemical characterisation, source apportionment and new marker identification, *Atmos. Chem. Phys.*, 21, 10133–
678 10158, <https://doi.org/10.5194/acp-21-10133-2021>, 2021.
- 679 Chandra, B. P., and Sinha, V.: Contribution of post-harvest agricultural paddy residue fires in the NW Indo-
680 Gangetic Plain to ambient carcinogenic benzenoids, toxic isocyanic acid and carbon monoxide, *Environ. Int.*, 88,
681 187-197, <https://doi.org/10.1016/j.envint.2015.12.025>, 2016.
- 682 Chandra, B. P., Sinha, V., Hakkim, H., Kumar, A., Pawar, H., Mishra, A. K., Sharma, G., Pallavi, Garg, S., Ghude,
683 S. D., Chate, D. M., Pithani, P., Kulkarni, R., Jenamani, R. K., and Rajeevan, M.: Odd-even traffic rule
684 implementation during winter 2016 in Delhi did not reduce traffic emissions of VOCs, carbon dioxide, methane
685 and carbon monoxide, *Curr. Sci. India*114(6), 1318–1325, <https://www.jstor.org/stable/26797338>, 2018.
- 686 Chen, T., Zhang, P., Chu, B., Ma, Q., Ge, Y., Liu, J., and He, H.: Secondary organic aerosol formation from mixed
687 volatile organic compounds: Effect of RO₂ chemistry and precursor concentration, *npj Climate and Atmospheric*
688 *Science*, 5(1), 95. <https://doi.org/10.1038/s41612-022-00321-y>, 2022.
- 689 Chin, J.-Y., Godwin, C., Jia, C., Robins, T., Lewis, T., Parker, E., Max, P., and Batterman, S.: Concentrations and
690 risks of p-dichlorobenzene in indoor and outdoor air, *Indoor Air*, 23, 40–49, <https://doi.org/10.1111/j.1600-0668.2012.00796.x>, 2013.
- 692 Crippa, M., Guizzardi, D., Muntean, M., Schaaf, E., Monforti-Ferrario, F., Banja, M., Pagani, F. and Solazzo, E.:
693 EDGAR v6.1 global air pollutant emissions, European Commission, JRC129555, 2022.



694 Coherent market insight: <https://www.coherentmarketinsights.com/market-insight/methanethiol-market-6065/>
695 last access: 19 January 2024.

696 de Gouw, J. A., Gilman, J. B., Kim, S.-W., Lerner, B. M., IsaacmanVanWertz, G., McDonald, B. C., Warneke, C.,
697 Kuster, W. C., Lefer, B. L., Griffith, S. M., Dusanter, S., Stevens, P. S., and Stutz, J.: Chemistry of Volatile Organic
698 Compounds in the Los Angeles basin: Nighttime Removal of Alkenes and Determination of Emission Ratios, *J.*
699 *Geophys. Res.-Atmos.*, 122, 11843–11861, <https://doi.org/10.1002/2017JD027459>, 2017.

700 de Gouw, J., and Warneke, C. (2007).: Measurements of volatile organic compounds in the earth's atmosphere
701 using proton-transfer-reaction mass spectrometry, *Mass spectrom. rev.*, 26(2), 223-
702 257, <https://doi.org/10.1002/mas.20119>, 2007.

703 Dolgorouky, C., Gros, V., Sarda-Esteve, R., Sinha, V., Williams, J., Marchand, N., Sauvage, S., Poulain, L., Sciare,
704 J., and Bonsang, B.: Total OH reactivity measurements in Paris during the 2010 MEGAPOLI winter campaign,
705 *Atmos. Chem. Phys.*, 12, 9593–9612, <https://doi.org/10.5194/acp-12-9593-2012>, 2012.

706 Durmusoglu, E., Taspinar, F., and Karademir, A.: Health risk assessment of BTEX emissions in the landfill
707 environment, *J. Hazard. Mater.*, 176(1-3), 870-877, <https://doi.org/10.1016/j.jhazmat.2009.11.117>, 2010.

708 Espenship, M.F., Silva, L.K., Smith, M.M., Capella, K.M., Reese, C.M., Rasio, J.P., Woodford, A.M., Geldner,
709 N.B., Rey deCastro, B., and De Jesús, V.R.: Nitromethane exposure from tobacco smoke and diet in the US
710 population: NHANES, 2007–2012, *Environ. Sci. Technol.* 53 (4), 2134–2140.
711 <https://pubs.acs.org/doi/abs/10.1021/acs.est.8b05579>, 2019.

712 Fang, M., Zheng, M., Wang, F., To, K. L., Jaafar, A. B., and Tong, S. L.: The solvent-extractable organic
713 compounds in the Indonesia biomass burning aerosols–characterization studies, *Atmos. Environ.*, 33(5), 783-795,
714 [https://doi.org/10.1016/S1352-2310\(98\)00210-6](https://doi.org/10.1016/S1352-2310(98)00210-6), 1999.

715 Gani, S., Bhandari, S., Patel, K., Seraj, S., Soni, P., Arub, Z., Habib, G., Hildebrandt Ruiz, L., and Apte, J.S.:
716 Particle number concentrations and size distribution in a polluted megacity: the Delhi Aerosol Supersite study,
717 *Atmos. Chem. Phys.* 20, 8533–8549. <https://doi.org/10.5194/acp-20-8533-2020>, 2020.

718 Garg, S., Chandra, B. P., Sinha, V., Sarda-Esteve, R., Gros, V., and Sinha, B.: Limitation of the use of the
719 absorption angstrom exponent for source apportionment of equivalent black carbon: a case study from the North
720 West Indo-Gangetic Plain, *Environ. Sci. Technol.* 50(2), 814-824, <https://doi.org/10.1021/acs.est.5b03868>, 2016.

721 Garzón, J. P., Huertas, J. I., Magaña, M., Huertas, M. E., Cárdenas, B., Watanabe, T., Maeda, T., Wakamatsu, S.,
722 and Blanco, S.: Volatile organic compounds in the atmosphere of Mexico City, *Atmos. Environ.*, 119, 415–429,
723 <https://doi.org/10.1016/j.atmosenv.2015.08.014>, 2015.

724 Graus, M., Müller, M., and Hansel, A.: High resolution PTR-TOF: quantification and formula confirmation of
725 VOC in real time, *J. Am. Soc. Mass Spectr.*, 21(6), 1037-1044, <https://doi.org/10.1016/j.jasms.2010.02.006>, 2011.

726 Gros, V., Gaimoz, C., Herrmann, F., Custer, T., Williams, J., Bonsang, B., Sauvage, S., Locoge, N., d'Argouges,
727 O., Sarda-Esteve, R., and Sciare, J.: Volatile organic compounds sources in Paris in spring 2007. Part I: qualitative
728 analysis, *Environ. Chem.*, 8, 74–90, 2011.

729 Guttikunda, S. K., Dammalapati, S. K., Pradhan, G., Krishna, B., Jethva, H. T., and Jawahar, P.: What Is Polluting
730 Delhi's Air? A Review from 1990 to 2022, *Sustainability* 15(5), 4209; <https://doi.org/10.3390/su15054209>, 2023.

731 Hakkim, H., Kumar, A., Annadate, S., Sinha, B., and Sinha, V.: RTEII: A new high-resolution (0.1°× 0.1°) road
732 transport emission inventory for India of 74 speciated NMVOCs, CO, NO_x, NH₃, CH₄, CO₂, PM_{2.5} reveals



- 733 massive overestimation of NO_x and CO and missing nitromethane emissions by existing inventories, *Atmos.*
734 *Environ.*: X, 11, 100118, <https://doi.org/10.1016/j.aeaoa.2021.100118>, 2021.
- 735 Hakkim, H., Sinha, V., Chandra, B. P., Kumar, A., Mishra, A. K., Sinha, B., Sharma, G., Pawar, H., Sohpaal, B.,
736 Ghude, S.D., Pithani, P., Kulkarni, R., Jenamani, R.K., and Rajeevan, M.: Volatile organic compound
737 measurements point to fog-induced biomass burning feedback to air quality in the megacity of Delhi, *Sci. Total*
738 *Environ.*, 689, 295-304, <https://doi.org/10.1016/j.scitotenv.2019.06.438>, 2019.
- 739 Hatakeyama, S., and Akimoto, H.: Reactions of hydroxyl radicals with methanethiol, dimethyl sulfide, and
740 dimethyl disulfide in air, *J. Phy. Chem.*, 87(13), 2387-2395, 1983.
- 741 Hatch, L. E., Yokelson, R. J., Stockwell, C. E., Veres, P. R., Simpson, I. J., Blake, D. R., Orlando, J. J., and
742 Barsanti, K. C.: Multi-instrument comparison and compilation of non-methane organic gas emissions from
743 biomass burning and implications for smoke-derived secondary organic aerosol precursors, *Atmos. Chem. Phys.*,
744 17, 1471–1489, <https://doi.org/10.5194/acp-17-1471-2017>, 2017.
- 745 Hersbach, H., Bell, B., Berrisford, P., Biavati, G., Horányi, A., Muñoz Sabater, J., Nicolas, J., Peubey, C., Radu,
746 R., Rozum, I., Schepers, D., Simmons, A., Soci, C., Dee, D., and Thépaut, J-N. (2023): ERA5 hourly data on
747 single levels from 1940 to present. Copernicus Climate Change Service (C3S) Climate Data Store (CDS), DOI:
748 [10.24381/cds.adbb2d47](https://doi.org/10.24381/cds.adbb2d47) (Accessed on 15-12-2023)
- 749 Ho, S. S. H., Yu, J. Z., Chu, K. W. and Yeung, L. L.: Carbonyl Emissions from Commercial Cooking Sources in
750 Hong Kong, *J. Air Waste Manage. Assoc.*, 56, 1091–1098, <https://doi.org/10.1080/10473289.2006.10464532> ,
751 2006.
- 752 Holzinger, R., Warneke, C., Hansel, A., Jordan, A., Lindinger, W., Scharffe, D. H., Schade, G., and Crutzen, P. J.:
753 Biomass burn ing as a source of formaldehyde, acetaldehyde, methanol, ace tone, acetonitrile, and hydrogen
754 cyanide, *Geophys. Res. Lett.*, 26, 1161–1164, doi:[10.1029/1999gl900156](https://doi.org/10.1029/1999gl900156), 1999.
- 755 Hu, Y., Ma, J., Zhu, M., Zhao, Y., Peng, S., and Zhu, C.: Photochemical oxidation of o-dichlorobenzene in aqueous
756 solution by hydroxyl radicals from nitrous acid, *J. Photoch. Photobio. A*, 420, 113503,
757 <https://doi.org/10.1016/j.jphotochem.2021.113503>, 2021.
- 758 Jain, V., Tripathi, S.N., Tripathi, N., Sahu, L.K., Gaddamidi, S., Shukla, A.K., Bhattu, D., and Ganguly, D.:
759 Seasonal variability and source apportionment of non-methane VOCs using PTR-TOF-MS measurements in
760 Delhi, India, *Atmos. Environ.* 283, 119163, <https://doi.org/10.1016/j.atmosenv.2022.119163>, 2022.
- 761 Jordan, A., Haidacher, S., Hanel, G., Hartungen, E., Märk, L., Seehauser, H., Schottkowsky, R., Sulzer, P., and
762 Märk, T. D.: A high resolution and high sensitivity proton-transfer-reaction time-of-flight mass spectrometer (PTR-
763 TOF-MS), *Int. J. Mass Spectrom.*, 286, 122–128, <https://doi.org/10.1016/j.ijms.2009.07.005>, 2009.
- 764 Kadota, H., and Ishida, Y.: Production of volatile sulfur compounds by microorganisms. *Annu. Rev.*
765 *Microbiol.*, 26(1), 127-138, DOI: [10.1146/annurev.mi.26.100172.001015](https://doi.org/10.1146/annurev.mi.26.100172.001015), 1972.
- 766 Kawamura, K., Okuzawa, K., Aggarwal, S. G., Irie, H., Kanaya, Y., and Wang, Z.: Determination of gaseous and
767 particulate carbonyls (glycolaldehyde, hydroxyacetone, glyoxal, methylglyoxal, nonanal and decanal) in the
768 atmosphere at Mt. Tai, *Atmos. Chem. Phys.*, 13, 5369–5380, <https://doi.org/10.5194/acp-13-5369-2013>, 2013.
- 769 Keyword, M., Paton-Walsh, C., Lawrence, M. G., George, C., Formenti, P., Schofield, R., Cleugh, H., Borgford-
770 Parnell, N., and Capon, A.: Atmospheric goals for sustainable development, *Science*, 379(6629), 246-247.
771 doi:[10.1126/science.adg2495](https://doi.org/10.1126/science.adg2495), 2023.



- 772 Kim, K.: Emissions of reduced sulfur compounds (RSC) as a landfill gas (LFG): a comparative study of young
773 and old landfill facilities, *Atmos. Environ.* 40, 6567–6578, <https://doi.org/10.1016/j.atmosenv.2006.05.063>, 2006.
- 774 Komae, S., Sekiguchi, K., Suzuki, M., Nakayama, R., Namiki, N., and Kagi, N.: Secondary organic aerosol
775 formation from p-dichlorobenzene under indoor environmental conditions, *Build. and Environ.* 174, 106758,
776 <https://doi.org/10.1016/j.buildenv.2020.106758>, 2020.
- 777 Koss, A. R., Sekimoto, K., Gilman, J. B., Selimovic, V., Coggon, M. M., Zarzana, K. J., Yuan, B., Lerner, B. M.,
778 Brown, S. S., Jimenez, J. L., Krechmer, J., Roberts, J. M., Warneke, C., Yokelson, R. J., and de Gouw, J.: Non-
779 methane organic gas emissions from biomass burning: identification, quantification, and emission factors from
780 PTR-ToF during the FIREX 2016 laboratory experiment, *Atmos. Chem. Phys.*, 18, 3299–3319,
781 <https://doi.org/10.5194/acp-18-3299-2018>, 2018.
- 782 Kulkarni, S.H., Ghude, S.D., Jena, C., Karumuri, R.K., Sinha, B., Sinha, V., Kumar, R., Soni, V.K., Khare, M.:
783 How much does large-scale crop residue burning affect the air quality in Delhi?, *Environ. Sci. Technol.* 54 (8),
784 4790–4799, <https://doi.org/10.1021/acs.est.0c00329>, 2020.
- 785 Kumar, A., Hakkim, H., Sinha, B., and Sinha, V.: Gridded 1 km \times 1 km emission inventory for paddy stubble
786 burning emissions over north-west India constrained by measured emission factors of 77 VOCs and district-wise
787 crop yield data, *Sci. Total Environ.*, 789, 148064, <https://doi.org/10.1016/j.scitotenv.2021.148064>, 2021.
- 788 Kumar, A., Sinha, V., Shabin, M., Hakkim, H., Bonsang, B., and Gros, V.: Non-methane hydrocarbon (NMHC)
789 fingerprints of major urban and agricultural emission sources for use in source apportionment studies, *Atmos.*
790 *Chem. Phys.*, 20, 12133–12152, <https://doi.org/10.5194/acp-20-12133-2020>, 2020.
- 791 Kumar, V., Chandra, B. P., and Sinha, V.: Large unexplained suite of chemically reactive compounds present in
792 ambient air due to biomass fires, *Sci. Rep.*, 8(1), 626, <https://doi.org/10.1038/s41598-017-19139-3>, 2018.
- 793 Kumar, V., Sarkar, C., and Sinha, V.: Influence of post-harvest crop residue fires on surface ozone mixing ratios
794 in the NW IGP analyzed using 2 years of continuous in situ trace gas measurements, *J. Geophys. Res.-Atmos.*,
795 121(7), 3619–3633, <https://doi.org/10.1002/2015JD024308>, 2016.
- 796 Kurokawa, J., and Ohara, T.: Long-term historical trends in air pollutant emissions in Asia: Regional Emission
797 inventory in ASia (REAS) version 3, *Atmos. Chem. Phys.*, 20(21), 12761–12793, <https://doi.org/10.5194/ACP-20-12761-2020>, 2020.
- 799 Langford, B., Nemitz, E., House, E., Phillips, G. J., Famulari, D., Davison, B., Hopkins, J. R., Lewis, A. C., and
800 Hewitt, C. N.: Fluxes and concentrations of volatile organic compounds above central London, UK, *Atmos. Chem.*
801 *Phys.*, 10, 627–645, <https://doi.org/10.5194/acp-10-627-2010>, 2010.
- 802 Lelieveld, J., Evans, J.S., Fnais, M., Giannadaki, D., and Pozzer, A.: The contribution of outdoor air pollution
803 sources to premature mortality on a global scale, *Nature* 525, 367–371, <https://doi.org/10.1038/nature15371>, 2015.
- 804 Li, K., Li, J., Tong, S., Wang, W., Huang, R.-J., and Ge, M.: Characteristics of wintertime VOCs in suburban and
805 urban Beijing: concentrations, emission ratios, and festival effects, *Atmos. Chem. Phys.*, 19, 8021–8036,
806 <https://doi.org/10.5194/acp-19-8021-2019>, 2019.
- 807 Lin, P., Liu, J., Shilling, J. E., Kathmann, S. M., Laskin J., and Laskin, A.: Molecular characterization of brown
808 carbon (BrC) chromophores in secondary organic aerosol generated from photo-oxidation of toluene,
809 *Phys.Chem.Chem.Phys.* 17, 23312–23325, <https://doi.org/10.1039/c5cp02563j>, 2015.



- 810 Lin, P., Bluvshstein, N., Rudich, Y., Nizkorodov, S. A., Laskin, J., and Laskin, A.: Molecular Chemistry of
811 Atmospheric Brown Carbon Inferred from a Nationwide Biomass Burning Event, *Environ. Sci. Technol.* 51(20),
812 11561–11570, <https://doi.org/10.1021/acs.est.7b02276>, 2017.
- 813 Mackay, D., Shiu, W. Y., and Ma, K. C.: Illustrated handbook of physical-chemical properties of environmental
814 fate for organic chemicals (Vol. 5). CRC press. 832pp., ISBN 978-1-56670-255-3, 1997.
- 815 McDonald, B.C., de Gouw, J.A., Gilman, J.B., Jathar, S.H., Akherati, A., Cappa, C.D., Jimenez, J.L., Lee-Taylor,
816 J., Hayes, P.L., McKeen, S.A., Cui, Y.Y., Kim, S.W., Gentner, D.R., Isaacman-VanWertz, G., Goldstein, A.H.,
817 Harley, R.A., Frost, G.J., Roberts, J.M., Ryerson, T.B., and Trainer, M.: Volatile chemical products emerging as
818 largest petrochemical source of urban organic emissions, *Science* 359, 760e764,
819 <https://doi.org/10.1126/science.aag0524>, 2018.
- 820 Millet, D. B., Guenther, A., Siegel, D. A., Nelson, N. B., Singh, H. B., de Gouw, J. A., Warneke, C., Williams, J.,
821 Eerdeken, G., Sinha, V., Karl, T., Flocke, F., Apel, E., Riemer, D. D., Palmer, P. I., and Barkley, M.: Global
822 atmospheric budget of acetaldehyde: 3-D model analysis and constraints from in-situ and satellite observations,
823 *Atmos. Chem. Phys.*, 10, 3405–3425, <https://doi.org/10.5194/acp-10-3405-2010>, 2010.
- 824 Mishra, A. K., and Sinha, V.: Emission drivers and variability of ambient isoprene, formaldehyde and acetaldehyde
825 in north-west India during monsoon season, *Environ. Pollut.*, 267, 115538,
826 <https://doi.org/10.1016/j.envpol.2020.115538>, 2020.
- 827 Nault, B. A., Jo, D. S., McDonald, B. C., Campuzano-Jost, P., Day, D. A., Hu, W., Schroder, J. C., Allan, J., Blake,
828 D. R., Canagaratna, M. R., Coe, H., Coggon, M. M., DeCarlo, P. F., Diskin, G. S., Dunmore, R., Flocke, F., Fried,
829 A., Gilman, J. B., Gkatzelis, G., Hamilton, J. F., Hanisco, T. F., Hayes, P. L., Henze, D. K., Hodzic, A., Hopkins,
830 J., Hu, M., Huey, L. G., Jobson, B. T., Kuster, W. C., Lewis, A., Li, M., Liao, J., Nawaz, M. O., Pollack, I. B.,
831 Peischl, J., Rappenglück, B., Reeves, C. E., Richter, D., Roberts, J. M., Ryerson, T. B., Shao, M., Sommers, J. M.,
832 Walega, J., Warneke, C., Weibring, P., Wolfe, G. M., Young, D. E., Yuan, B., Zhang, Q., de Gouw, J. A., and
833 Jimenez, J. L.: Secondary organic aerosols from anthropogenic volatile organic compounds contribute
834 substantially to air pollution mortality, *Atmos. Chem. Phys.*, 21, 11201–11224, <https://doi.org/10.5194/acp-21-11201-2021>, 2021.
- 836 Nelson, B. S., Stewart, G. J., Drysdale, W. S., Newland, M. J., Vaughan, A. R., Dunmore, R. E., Edwards, P. M.,
837 Lewis, A. C., Hamilton, J. F., Acton, W. J., Hewitt, C. N., Crilley, L. R., Alam, M. S., Şahin, Ü. A., Beddows, D.
838 C. S., Bloss, W. J., Slater, E., Whalley, L. K., Heard, D. E., Cash, J. M., Langford, B., Nemitz, E., Sommariva, R.,
839 Cox, S., Shivani, Gadi, R., Gurjar, B. R., Hopkins, J. R., Rickard, A. R., and Lee, J. D.: In situ ozone production
840 is highly sensitive to volatile organic compounds in Delhi, India, *Atmos. Chem. Phys.*, 21, 13609–13630,
841 <https://doi.org/10.5194/acp-21-13609-2021>, 2021.
- 842 Nielsen, C. J., Herrmann, H., and Weller, C.: Atmospheric chemistry and environmental impact of the use of
843 amines in carbon capture and storage (CCS), *Chemical Society Reviews*, 41(19), 6684-6704,
844 <https://doi.org/10.1039/C2CS35059A>, 2012.
- 845 Nunes, L.S., Tavares, T.M., Dippel, J., and Jaeschke, W.: Measurements of Atmospheric Concentrations of
846 Reduced Sulphur Compounds in the All Saints Bay Area in Bahia, Brazil, *J. Atmos. Chem.*, 50, 79-100,
847 <https://doi.org/10.1007/s10874-005-3123-0>, 2005.



- 848 Oros, D. R., bin Abas, M. R., Omar, N. Y. M., Rahman, N. A., and Simoneit, B. R.: Identification and emission
849 factors of molecular tracers in organic aerosols from biomass burning: Part 3. Grasses, *Appl. Geochem.* 21(6),
850 919-940, <https://doi.org/10.1016/j.apgeochem.2006.01.008>, 2006.
- 851 Pagonis, D., Sekimoto, K., and de Gouw, J.: A library of proton-transfer reactions of H₃O⁺ ions used for trace gas
852 detection, *J. Am. Soc. Mass Spectr.*, 30(7), 1330-1335, <https://doi.org/10.1007/s13361-019-02209-3>, 2019.
- 853 Pawar, H., Garg, S., Kumar, V., Sachan, H., Arya, R., Sarkar, C., Chandra, B. P., and Sinha, B.: Quantifying the
854 contribution of long-range transport to particulate matter (PM) mass loadings at a suburban site in the north-
855 western Indo-Gangetic Plain (NW-IGP), *Atmos. Chem. Phys.*, 15, 9501–9520, <https://doi.org/10.5194/acp-15-9501-2015>, 2015.
- 857 Pawar, P. V., Ghude, S. D., Govardhan, G., Acharja, P., Kulkarni, R., Kumar, R., Sinha, B., Sinha, V., Jena, C.,
858 Gunwani, P., Adhya, T. K., Nemitz, E., and Sutton, M. A.: Chloride (HCl/Cl⁻) dominates inorganic aerosol
859 formation from ammonia in the Indo-Gangetic Plain during winter: modeling and comparison with observations,
860 *Atmos. Chem. Phys.*, 23, 41–59, <https://doi.org/10.5194/acp-23-41-2023>, 2023.
- 861 Piel, F., Müller, M., Winkler, K., Skytte af Sättra, J., and Wisthaler, A.: Introducing the extended volatility range
862 proton-transfer-reaction mass spectrometer (EVR PTR-MS), *Atmos. Meas. Tech.*, 14, 1355–1363,
863 <https://doi.org/10.5194/amt-14-1355-2021>, 2021.
- 864 Reed, N. W., Browne, E. C., and Tolbert, M. A.: Impact of hydrogen sulfide on photochemical haze formation in
865 methane/nitrogen atmospheres, *ACS Earth and Space Chemistry*, 4(6), 897-904,
866 <https://doi.org/10.1021/acsearthspacechem.0c00086>, 2020.
- 867 Roberts, J. M., Veres, P. R., Cochran, A. K., Warneke, C., Burling, I. R., Yokelson, R. J., Lerner, B., Gilman, J. B.,
868 Kuster, W. C., Fall, R., and de Gouw, J.: Isocyanic acid in the atmosphere and its possible link to smoke-related
869 health effects, *Proc. Natl. Acad. Sci. USA*, 108, 8966–8971, <https://doi.org/10.1073/pnas.1103352108>, 2011.
- 870 Sarkar, C., Sinha, V., Kumar, V., Rupakheti, M., Panday, A., Mahata, K. S., Rupakheti, D., Kathayat, B., and
871 Lawrence, M. G.: Overview of VOC emissions and chemistry from PTR-TOF-MS measurements during the
872 SusKat-ABC campaign: high acetaldehyde, isoprene and isocyanic acid in wintertime air of the Kathmandu
873 Valley, *Atmos. Chem. Phys.*, 16, 3979–4003, <https://doi.org/10.5194/acp-16-3979-2016>, 2016.
- 874 Sharma, S. K., and Mandal, T. K.: Elemental composition and sources of fine particulate matter (PM_{2.5}) in Delhi,
875 India, *Bulletin of Environmental Contamination and Toxicology*, 110(3), 60. <https://doi.org/10.1007/s00128-023-03707-7>, 2023.
- 877 Singh, D. P., Gadi, R., and Mandal, T. K.: Characterization of particulate-bound polycyclic aromatic hydrocarbons
878 and trace metals composition of urban air in Delhi, India, *Atmos. Environ.*, 45(40), 7653-7663,
879 <https://doi.org/10.1016/j.atmosenv.2011.02.058>, 2011.
- 880 Singh, R., Sinha, B., Hakkim, H., and Sinha, V.: Source apportionment of volatile organic compounds during
881 paddy-residue burning season in north-west India reveals large pool of photochemically formed air
882 toxics, *Environ. Pollut.*, 338, 122656, <https://doi.org/10.1016/j.envpol.2023.122656>, 2023.
- 883 Sinha, V., Kumar, V., and Sarkar, C.: Chemical composition of pre-monsoon air in the Indo-Gangetic Plain
884 measured using a new air quality facility and PTR-MS: high surface ozone and strong influence of biomass
885 burning, *Atmos. Chem. Phys.*, 14, 5921–5941, <https://doi.org/10.5194/acp-14-5921-2014>, 2014.
- 886 Stark, H., Yatavelli, R. L. N., Thompson, S. L., Kimmel, J. R., Cubison, M. J., Chhabra, P. S., Canagaratna, M.
887 R., Jayne, J. T., Worsnop, D. R., and Jimenez, J. L.: Methods to extract molecular and bulk chemical information



888 from series of complex mass spectra with limited mass resolution, *Int. J. Mass Spectrom.*, 389, 26–38,
889 <https://doi.org/10.1016/j.ijms.2015.08.011>, 2015.

890 Stockwell, C. E., Veres, P. R., Williams, J., and Yokelson, R. J.: Characterization of biomass burning emissions
891 from cooking fires, peat, crop residue, and other fuels with high-resolution proton-transfer-reaction time-of-flight
892 mass spectrometry, *Atmos. Chem. Phys.*, 15, 845–865, <https://doi.org/10.5194/acp-15-845-2015>, 2015.

893 Toda, K., Obata, T., Obokin, V. A., Potemkin, V. L., Hirota, K., Takeuchi, M., Arita, S., Khodzher, T. V., and
894 Grachev, M. A.: Atmospheric methanethiol emitted from a pulp and paper plant on the shore of Lake Baikal,
895 *Atmos. Environ.*, 44, 2427–2433, doi:[10.1016/j.atmosenv.2010.03.037](https://doi.org/10.1016/j.atmosenv.2010.03.037), 2010.

896 Tripathi, N., Sahu, L. K., Wang, L., Vats, P., Soni, M., Kumar, P., Satish, R. V., Bhattu, D., Sahu, R., Patel, K.,
897 Rai, P., Kumar, V., Rastogi, N., Ojha, N., Tiwari, S., Ganguly, D., Slowik, J., Prévôt, A. S. H., and Tripathi, S. N.:
898 Characteristics of VOC Composition at Urban and Suburban Sites of New Delhi, India in Winter, *J. Geophys.*
899 *Res.-Atmos.*, 127, e2021JD035342, <https://doi.org/10.1029/2021JD035342>, 2022.

900 Valach, A. C., Langford, B., Nemitz, E., MacKenzie, A. R., and Hewitt, C. N.: Concentrations of selected volatile
901 organic compounds at kerbside and background sites in central London, *Atmos. Environ.*, 95, 456–467,
902 <https://doi.org/10.1016/j.atmosenv.2014.06.052>, 2014.

903 Wang, M., Shao, M., Chen, W., Yuan, B., Lu, S., Zhang, Q., Zeng, L., and Wang, Q.: A temporally and spatially
904 resolved validation of emission inventories by measurements of ambient volatile organic compounds in Beijing,
905 China, *Atmos. Chem. Phys.*, 14, 5871–5891, <https://doi.org/10.5194/acp-14-5871-2014>, 2014.

906 Wang, L., Slowik, J. G., Tripathi, N., Bhattu, D., Rai, P., Kumar, V., Vats, P., Satish, R., Baltensperger, U., Ganguly,
907 D., Rastogi, N., Sahu, L. K., Tripathi, S. N., and Prévôt, A. S. H.: Source characterization of volatile organic
908 compounds measured by proton-transfer-reaction time-of-flight mass spectrometers in Delhi, India, *Atmos. Chem.*
909 *Phys.*, 20, 9753–9770, <https://doi.org/10.5194/acp-20-9753-2020>, 2020.

910 Warneke, C., Holzinger, R., Hansel, A., Jordan, A., Lindinger, W., Pöschl, U., Williams, J., Hoor, P., Fischer, H.,
911 Crutzen, P.J., Scheeren, H.A., and Lelieveld, J.: Isoprene and its oxidation products methyl vinyl ketone,
912 methacrolein, and isoprene related peroxides measured online over the tropical rain forest of Surinam in March
913 1998, *J. Atmos. Chem.*, 38, 167–185, <https://doi.org/10.1023/A:1006326802432>, 2001.

914 Warneke, C., McKeen, S. A., de Gouw, J. A., Goldan, P. D., Kuster, W. C., Holloway, J. S., Williams, E. J., Lerner,
915 B. M., Parrish, D. D., Trainer, M., Fehsenfeld, F. C., Kato, S., Atlas, E. L., Baker, A., and Blake, D. R.:
916 Determination of urban volatile organic compound emission ratios and comparison with an emissions database,
917 *J. Geophys. Res.*, 112, D10S47, <https://doi.org/10.1029/2006JD007930>, 2007.

918 Weng, M., Zhu, L., Yang, K., and Chen, S.: Levels and health risks of carbonyl compounds in selected public
919 places in Hangzhou, China, *J. Hazard. Mater.*, 164(2-3), 700-706, <https://doi.org/10.1016/j.jhazmat.2008.08.094>,
920 2009.

921 WHO Guidelines for Indoor Air Quality: Selected Pollutants, edited by: Theakston, F., World Health Organization:
922 WHO Regional Office for Europe, Copenhagen, Denmark, 1–454, 2010.

923 WHO 2019.: Exposure to benzene: a major public health concern: [https://www.who.int/publications/i/item/WHO-](https://www.who.int/publications/i/item/WHO-CED-PHE-EPE-19.4.2)
924 [CED-PHE-EPE-19.4.2](https://www.who.int/publications/i/item/WHO-CED-PHE-EPE-19.4.2), last access: 19 January 2024.

925 Wine, P. H., Kreutter, N. M., Gump, C. A., and Ravishankara, A. R.: Kinetics of hydroxyl radical reactions with
926 the atmospheric sulfur compounds hydrogen sulfide, methanethiol, ethanethiol, and dimethyl disulfide, *J. Phys.*
927 *Chem.*, 85(18), 2660-2665, 1981.



- 928 Yáñez-Serrano, A. M., Filella, I., LLusià, J., Gargallo-Garriga, A., Granda, V., Bourtsoukidis, E., Williams, J.,
929 Seco, R., Cappellin, L., Werner, C., de Gouw, J., and Peñuelas, J.: GLOVOCS - Master compound assignment
930 guide for proton transfer reaction mass spectrometry users, *Atmos. Environ.* 244, 117929,
931 <https://doi.org/10.1016/J.ATMOSENV.2020.117929>, 2021.
- 932 Yao, L., Wang, M.-Y., Wang, X.-K., Liu, Y.-J., Chen, H.-F., Zheng, J., Nie, W., Ding, A.-J., Geng, F.-H., Wang,
933 D.-F., Chen, J.-M., Worsnop, D. R., and Wang, L.: Detection of atmospheric gaseous amines and amides by a
934 high-resolution time-of-flight chemical ionization mass spectrometer with protonated ethanol reagent ions, *Atmos.*
935 *Chem. Phys.*, 16, 14527–14543, <https://doi.org/10.5194/acp-16-14527-2016>, 2016.
- 936 Yoshino, A., Nakashima, Y., Miyazaki, K., Kato, S., Suthawaree, J., Shimo, N., Matsunaga, S., Chatani, S., Apel,
937 E., Greenberg, J., Guenther, A., Ueno, H., Sasaki, H., Hoshi, J. Y., Yokota, H., Ishii, K., and Kajii, Y.: Air quality
938 diagnosis from comprehensive observations of total OH reactivity and reactive trace species in urban central
939 Tokyo, *Atmos. Environ.*, 49, 51–59, doi:[10.1016/j.atmosenv.2011.12.029](https://doi.org/10.1016/j.atmosenv.2011.12.029), 2012.
- 940 Yuan, B., Koss, A.R., Warneke, C., Coggon, M., Sekimoto, K., and de Gouw, J.: Proton-Transfer Reaction Mass
941 Spectrometry: Applications in Atmospheric Sciences, *Chem. Rev.* 117 (21), 13187-13229,
942 <https://doi.org/10.1021/acs.chemrev.7b00325>, 2017.
- 943 Zhou, X., Li, Z., Zhang, T., Wang, F., Wang, F., Tao, Y., Zhang, X., Wang, F., and Huang, J.: Volatile organic
944 compounds in a typical petrochemical industrialized valley city of northwest China based on high-resolution PTR-
945 MS measurements: Characterization, sources and chemical effects, *Sci. Total Environ.*, 671, 883– 896,
946 <https://doi.org/10.1016/j.scitotenv.2019.03.283>, 2019.
- 947